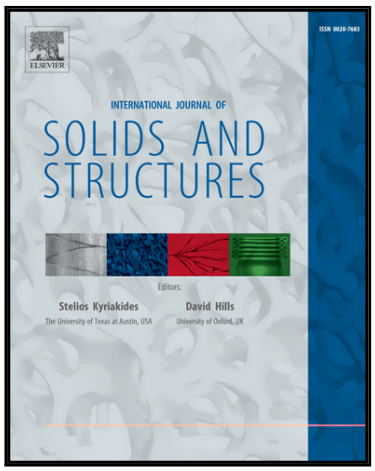

Universal analytical solution of the steady-state response of an infinite beam on a Pasternak elastic foundation under moving load

Diego Froio, Egidio Rizzi, Fernando M.F. Simões, António Into Da Costa

PII: S0020-7683(17)30467-5
DOI: 10.1016/j.ijsolstr.2017.10.005
Reference: SAS 9757

To appear in: *International Journal of Solids and Structures*

Received date: 5 October 2016
Revised date: 29 September 2017
Accepted date: 5 October 2017

Please cite this article as: Diego Froio, Egidio Rizzi, Fernando M.F. Simões, António Into Da Costa, Universal analytical solution of the steady-state response of an infinite beam on a Pasternak elastic foundation under moving load, *International Journal of Solids and Structures* (2017), doi: 10.1016/j.ijsolstr.2017.10.005

Highlights

- Exact derivation by Fourier transform of a universal, explicit closed-form parametric analytical solution of the steady-state response of a uniform infinite Euler-Bernoulli elastic beam on a Pasternak elastic foundation subjected to a concentrated load moving at constant velocity.
- Rigorous mathematical procedure for classification of the parametric behavior of the solution, by varying the mechanical parameters of the beam-foundation system, based on the parametric nature of the Fourier transform poles.
- Different types of bending wave shapes are shown to propagate within the beam, including for new solution instances that may be obtained for given values of the physical parameters, such as for a high Pasternak modulus.
- Original re-derivation and reinterpretation of steady-state physical characteristics, such as critical velocity and two-branch critical damping.
- Highlighting of characteristic features of the physical steady-state response by a parametric analysis involving normalized deflection, cross-section rotation, bending moment and shear force.

Universal analytical solution of the steady-state response of an infinite beam on a Pasternak elastic foundation under moving load

Diego FROIO[1], Egidio RIZZI[1]*,
Fernando M.F. SIMÕES[2], António PINTO DA COSTA[2]

[1] *Dipartimento di Ingegneria e Scienze Applicate, Università degli Studi di Bergamo, viale G. Marconi 5, I-24044 Dalmine (BG), Italy*

[2] *CERIS, Instituto Superior Técnico, Universidade de Lisboa, Avenida Rovisco Pais, 1049-001 Lisboa, Portugal*

Abstract

In this paper, the steady-state response of a uniform infinite Euler-Bernoulli elastic beam resting on a Pasternak elastic foundation and subjected to a concentrated load moving at a constant velocity along the beam is analytically investigated. A universal closed-form analytical solution is derived through Fourier transform, apt to represent the response for all possible beam-foundation parameters. A rigorous mathematical procedure is formulated for classifying the parametric behavior of the solution, including for viscous damping. Depending on such a classification, different types of bending wave shapes are shown to propagate within the beam, ahead and behind the moving load position, and crucial physical characteristics, such as critical velocity and critical damping, are reinterpreted into a wholly exact and complete mathematical framework. Mechanical features of the solution are revealed for the steady-state response in terms of normalized deflection, cross-section rotation, bending moment and shear force.

Keywords: Moving Load; Beam on Pasternak support; Steady-state response; Universal closed-from analytical solution; Classification of all solutions; Critical velocity and critical damping.

1 Introduction

1.1 General framework and contextualization

Dynamic response and wave propagation phenomena under moving loads constitute a classical research topic referring to many important engineering applications, such as in railway and transportation engineering, e.g. in the construction of railroad tracks, roads and concrete pavements, rocket testing facilities (e.g. Kenney (1954) [1]) and ice plates (on this specific case see e.g. Schulkes and Sneyd (1988) [2] and Squire et al. (1996) [3]).

*Corresponding Author, egidio.rizzi@unibg.it, University of Bergamo, Department of Engineering and Applied Sciences (Dalmine), viale G. Marconi 5, I-24044 Dalmine (BG), Italy.
Tel: +39.035.205.2325; Fax: +39.035.205.2310.
E-mails: diego.froio@unibg.it (D. Froio), egidio.rizzi@unibg.it (E. Rizzi), fernando.simoes@tecnico.ulisboa.pt (F.M.F. Simões), antonio.pinto.da.costa@tecnico.ulisboa.pt (A. Pinto da Costa).

Structural vibrations induced by a moving load may become very high, when the velocity of the moving load attains a certain characteristic value, referred to as *critical velocity*, which, for an infinite beam, corresponds to the minimum phase velocity of the bending wave propagating within the beam-support system (see e.g. Kenney (1954) [1]) while, for finite beams, it is the lowest between the modal resonant velocities (Dimitrovová and Rodrigues (2012) [4]). In this latter paper, the developed analysis is not connected to finite beams only, but it includes infinite beams as well, abrupt changes in foundation stiffness and critical velocity/damping formulas are presented also for a Timoshenko beam.

In the last few decades, numerous research works have been presented, with the majority of them considering a "moving load" problem, i.e. the problem of a single load traveling at a constant velocity along a beam, usually supported by an elastic foundation, thus neglecting inertial effects due to the mass of the supporting medium and considering wave propagation just within the supported structure. The "moving mass" problem, instead, has been studied by several authors; among those, noteworthy to mention are the works of Duffy (1990) [5], Metrikine and Dieterman (1997) [6], Dimitrovová (2017) [7].

Comprehensive literature reviews about beams under moving loads may be found in Frýba (1972)[8], Kerr (1981) [9], Ouyang (2011) [10] and Beskou and Theodorakopoulos (2011) [11]. An analytical approach to the steady-state response of a beam/plate structural system on a Winkler viscoelastic foundation under moving load has been formulated in Shamalta and Metrikine (2003) [12]. Attempts in the FEM modelization of the moving load problem have been also developed in the recent literature (see e.g. Castro et al. (2014) [13], Castro et al. (2014) [14] and references quoted therein).

Further, most accurate models could even consider wave propagation phenomena in both beam and underlying substratum, described as a continuum of a finite depth, leading to an even more comprehensive description in terms of characteristic features, like for the critical velocity of passing trains, as very recently proven by Dimitrovová (2016,2017) [15, 16].

Kenney (1954) [1] solved the case of an infinitely long Euler-Bernoulli elastic beam lying on a Winkler elastic foundation. In the Winkler model, the support is represented by a set of continuously-distributed, non-interconnected springs with a locally-constant stiffness (see e.g. Froio and Rizzi (2016) [18], containing also an historical perspective review, and Froio and Rizzi (2017) [19]). Kenney (1954) [1] derived the analytical solution of the steady-state response for a constant-velocity moving load, by using a Green's function approach, accounting for viscous damping. According to the theory of harmonic flexural waves (see e.g. Graff (1975) [20]), the velocity of propagation of free waves for the undamped case was obtained. Furthermore, it was shown that if the velocity of the traveling load becomes equal to such a free wave or group velocity, displacements increase boundlessly, in the limit case of no damping, resulting in a resonance condition. In fact, as exposed by Simkins (1989) [21] for the analysis of gun tubes, the wave energy, which is transferred at the group velocity, concentrates on the load front (phase velocity) and continuously builds up the deformation near the front, as time progresses. Kenney (1954) [1]

also showed that for a load velocity lower than the critical velocity (subcritical case), the largest wave amplitude occurs near the loading point, while, for a load velocity larger than the critical one (supercritical case), the waves moving ahead of the load become smaller in amplitude and in wavelength than those behind the load.

Mathews (1958) [24] and Achenbach and Sun (1965) [22] generalized Kenney's analytical solution for a moving load with harmonically varying amplitude and for a Timoshenko beam, respectively; a similar set of equations was derived by Jones and Buta (1964) [23], by investigating the steady-state response of cylindrical shells to a moving ring load. Chen et al. (2001) [26] obtained the bifurcation curves of the critical velocities in case of a harmonic moving load acting on an infinite compressed Timoshenko beam by using the dynamic stiffness method. In that context, Froio et al. (2016) [25] have developed a FEM approach to characterize such bifurcation curves for a nonlinear support.

1.2 Pasternak foundation studies

A fundamental limitation of the Winkler elastic foundation model is that of neglecting the interactions between adjacent foundation springs, thus overlooking for the cohesive bonds between medium particles. This may lead to unrealistic results (Limkatanyu et al. (2015) [28]). To narrow down the gap between the real behaviour of continuous media and Winkler elastic foundation models, several researchers have enriched the Winkler model by introducing a coupling effect between continuous Winkler springs and different embedded structural elements. Among these models, the Pasternak one accounts for the existence of a shear interaction between the spring elements, by connecting the top end of each spring to an incompressible layer, which deforms under transverse shear and whose shear elastic modulus dictates the amount of shear coupling between neighboring springs (Selvadurai (1979) [29]). For this reason, this model is often classified as a "two-parameter" foundation model, where the first parameter represents the vertical stiffness of the foundation springs, like in a classical Winkler model, while the second parameter accounts for their shear coupling. The simplified continuum analysis by Vlasov and Leontiev (1966) [30] showed that the mechanical behavior of an elastic continuum can be simulated by using springs with such a shear-type interaction.

Kerr (1972) [27], a main reference in the present mathematical framing of the underlying differential problem, has studied the effect of a compression axial force on an *undamped* beam-foundation system, which may be induced by a rise in temperature within the beam. It is shown that the action of the compression force progressively decreases to zero the value of the critical velocity, when it reaches the critical static buckling load of an infinite beam. In this sense, though the essence of that structural problem is different than that considered here, the action of a compression force in softening the model is analogous to the effect of the Pasternak foundation in strengthening the model.

A formal integral solution of the general dynamic problem of the transient and steady-state vibrations of an infinite Euler-Bernoulli beam on an elastic foundation has been

obtained by both Stadler and Shreeves (1970) [31] and Sheehan and Debnath (1972) [32], by applying the joint Laplace and Fourier transforms. By assuming the beam as a two-dimensional elastic continuum, Saito and Terasawa (1981) [33] derived the equations of motion of an elastic infinite beam supported by a Pasternak-type foundation and subjected to a moving load distributed on a narrow finite length. The Fourier transform technique was applied to compute the steady-state response, even though no analytical formulation of the solution was present. Numerical results revealed unimportant discrepancies between the two-dimensional elastic theory and the Euler-Bernoulli and Timoshenko beam theories.

The response of a uniform Timoshenko beam of infinite length placed on a generalized Pasternak viscoelastic foundation and subjected to a harmonic arbitrary distributed moving load was computed numerically by Kargarnovin and Younesian (2004) [34] by using the Fourier transform coupled with the Gaussian quadrature method. In a subsequent work, Younesian and Kargarnovin (2009) [35] considered the same problem, but with a stochastic variation of the Winkler modulus along the beam axis. Nonlinear problems involving an infinite beam on a Pasternak foundation seem rather limited in the literature; one example may be found in the work of Ding et al. (2013) [36], where the Adomian Decomposition method was applied to determine the dynamic response of the beam.

Regarding the steady-state response of infinite elastic plates on an elastic support under moving load, the interested reader may be referred to the works of Stadler (1971) [37] and of Watanabe (1981) [38]. Stadler (1971) [37] considered a Winkler support and derived the analytical solution of the steady-state response of the plate in integral form by using the Fourier transform. On the other hand, the problem of an elastic plate resting on an undamped Pasternak foundation under a concentrated load moving at a constant velocity along a straight line was analyzed by Watanabe (1981) [38]. By applying the double Fourier transform, the author derived a formal integral expression of the solution, by means of which he finally numerically computed the plate response. Thus, such a representation is not fully explicit in analytical terms and anyhow neglects the role of damping.

1.3 Present developments on analytical steady-state response

In the present paper, a homogeneous infinite Euler-Bernoulli elastic beam of constant cross-section resting on a uniform Pasternak elastic foundation is considered. Smeared structural viscous damping is accounted for. The beam is subjected to a constant point load moving with a constant velocity along the beam. A steady-state solution response is sought, derived and interpreted in terms of all the involved characteristic structural parameters of the beam-foundation system. After the general premises above, detailed analytical studies directly related to the specific subject of the present work are briefly discussed below, to further motivate the problem statement, to outline the developed method for the analytical solution and to highlight the differences and novelties of the present work with respect to such previous important research contributions.

Some authors have derived the analytical solution for the steady-state vibrations of

an infinite beam on a Pasternak foundation, in analogy with the analysis proposed by Kenney (1954) [1] and Kerr (1972) [27]. Mallik et al. (2006) [39] and Basu and Kameswara Rao (2013) [40] based their derivation on a priori assuming an exponential form of the solution, while a Fourier transform technique was employed by Cao and Zhong (2008) [41] and Uzzal et al. (2012) [42], to find out the analytical solution for some solution cases. A purely numerical approach based of a Fast Fourier Transform technique (FFT) was instead employed by Evcan and Hayir (2013) [43], who analyzed numerically the undamped beam displacement response at subcritical moving load velocities.

In further details, Mallik et al. (2006) [39] derived the variation of the dynamic amplification factor of maximum settlement, uplift and bending moment of the beam as a function of load velocity, by evidencing an analogy with the frequency response curve of a SDOF system. The critical velocity of the beam-foundation system under moving load plays the same role of the resonance frequency of the SDOF system, leading to an unbounded response. In addition, the effect of viscous damping on the dynamic amplification factor becomes very similar in both cases.

Cao and Zhong (2008) [41] presented the effect of the velocity of the moving load and of the Pasternak modulus on the dynamic displacement response. In such a work, damping was not taken into account, and consequently only a subcritical range of velocities was considered, as in Evcan and Hayir (2013) [43]. The maximum deflection of the beam, placed always beneath the load, increased slightly at growing load velocity, and rather significantly by reducing the Pasternak modulus.

Parametric analyses were also obtained by Uzzal et al. (2012) [42], who described the variation of the beam deflections and of the bending moments with respect to different velocity ratios, Pasternak moduli and foundation stiffnesses. As a rather unexpected occurrence, the reported results seemed to display some differences with respect to the response earlier depicted by Mallik et al. (2006) [39].

Basu and Kameswara Rao (2013) [40] investigated deflection, bending moment, shear force and contact pressure for a load moving at subcritical and supercritical velocities, for different damping ratios. The dependence of the critical velocity and of the critical damping, i.e. the amount of damping for which the wavelength of the wave propagating behind the load becomes infinite, on the foundation parameters was also investigated.

Even though analytical and numerical solutions have been determined in the studies above, their application seems to have been limited to certain combinations of beam and foundation stiffness parameters, and some considered just the undamped case. For instance, no special importance was given to the consideration of a "large" Pasternak modulus $G_P > \sqrt{4kEJ}$, although this may apply to practical instances, since the stiffness of the beam or of the support may widely vary (see e.g. Razaqpur and Shah (1991) [44]). Instead, focusing also on the explicit inspection on large values of G_P brings further attention on a second branch of the critical damping curve (as depicted later in Fig. 6), each branch corresponding to a specific traveling wave pattern, shifting from propagating

to evanescent wave, either in front (left branch) or behind (right branch) the moving load position, thus highlighting an important feature of a complete analytical investigation.

In order to provide an analytical tool endowed of a general validity, *the objective of the present paper is to analyze all possible instances of the characteristic system parameters and to analytically derive a universal explicit formulation for the steady-state response, by a rigorous Fourier transform approach.* Through a complete mathematical treatment, a comprehensive classification of all solution cases is achieved in the paper, according to the values of the characteristic system parameters, which determine the nature of the poles of the Fourier transform of the solution. By virtue of such a classification, an a priori characterization about how the beam-foundation steady-state response shape changes according to the paths followed in the space of the system parameters, by varying load velocity, Pasternak shear modulus and damping coefficient, is developed. Characteristic features of the steady-state response such as critical velocity and critical damping are rigorously derived and interpreted. A unified analytical representation of the solution is also obtained and then adopted to plot, inspect and interpret the associated structural response.

The present analysis focuses on the various mathematical steps of the derivation and on their implications in the external manifestation of the achieved steady-state solution. The motivation of the present research work is to provide a whole complete and general solution, seemingly lacking in the several contributions dispersed in the literature, accounting all together for the presence of Pasternak modulus, structural viscous damping and the other characteristic mechanical parameters of the beam-foundation system, possibly varying over all their range of existence, thus becoming useful for reference and validation of numerical implementations of moving load problems (Eftekhari (2016) [45]), in all possible parameter and solution ranges. Such a derivation is conceived as to be rigorous and self-contained, so that the reader may follow all the truly needed steps. This has led to the main result of the paper, as condensed in the synoptic chart later shown in Fig. 4 (and solution regions in Fig. 2), complementing the previous contributions above. Such an achievement would allow readers to analytically plot and inspect the analytical solution, at variable system parameters (i.e. by independently reproducing the trends that will be depicted in following Figs. 8-12), without wondering much about the various underlying solution cases.

Presentation in the paper is organized as follows. Section 2 introduces the steady-state formulation of an infinite Euler-Bernoulli elastic beam resting on a Pasternak foundation. In Section 3, a complete Fourier transform approach developed for deriving the analytical solution is reported. In Section 4, after the determination of the general parametric form of the poles of the Fourier transform of the solution, the analytical solution is finally derived in exact closed form by inverting the Fourier transform, according to a universal solution representation. The singular cases of critical velocity and critical damping are also derived and analyzed. In Section 5, normalized curves of the complete steady-state response of the beam-foundation system (deflection, rotation, bending moment and shear force) are represented, and their dependence on the characteristic parameters of the dynamical

system is discussed. Finally, main conclusions are outlined in closing Section 6.

2 Steady-state problem formulation

2.1 Statement in non-dimensional variables and parameters

Consider an infinite Euler-Bernoulli elastic beam lying on a Pasternak viscoelastic foundation (Fig. 1), endowed with a fixed reference frame (x,y,z) and a time variable t. Positive beam cross-section rotations obey to the right-handed screw rule. A positive bending moment indicates tensile stresses in the bottom of the beam and positive shear indicates that the left side of the beam tends to rise. The infinite beam is traversed by a constant force F [N], positive if upward, moving from $-\infty$ to $+\infty$ at constant velocity v [m/s]. Load, taken upward for the derivation, will act downward in the final presented applications.

The equation of motion describing transverse deflection $w(x,t)$ [m] of the beam is represented by the following fourth-order Partial Differential Equation (PDE):

$$EJ\frac{\partial^4 w(x,t)}{\partial x^4} - G_P\frac{\partial^2 w(x,t)}{\partial x^2} + \mu\frac{\partial^2 w(x,t)}{\partial t^2} + c\frac{\partial w(x,t)}{\partial t} + kw(x,t) = F\delta(x-vt); \qquad (1)$$

where EJ [N m^2] and μ [kg/m] are elastic bending stiffness and mass per unit length of the beam, respectively; also, regarding the elastic foundation, k [N/m^2] and G_P [N] are Winkler and Pasternak foundation moduli, respectively (Wang et al. (2005) [17]); c is the viscous damping coefficient per unit length of the beam-foundation system [Ns/m^2]; all such characteristic parameters are assumed to be constant in both space and time variables. Finally, δ on the right-hand side of Eq. (1) is the Dirac delta function.

By assuming negligible transient effects, it is possible to directly correlate $w(x,t)$ to the character of forcing action $F\delta(x-vt)$ (steady-state conditions, see e.g. Kenney (1954) [1]):

$$w(x,t) = w_0\hat{w}(\lambda(x-vt)); \qquad (2)$$

where $\hat{w}$ is a dimensionless steady-state beam deflection, measured at locations $x-vt$ [m] relative to moving load position vt, w_0 [m] is a normalizing factor, to be defined later, and parameter λ [m]$^{-1}$ is the so-called wave number of the corresponding static problem (v=0), for a Winkler elastic foundation (G_P=0, see e.g. Hetényi (1946) [46]).

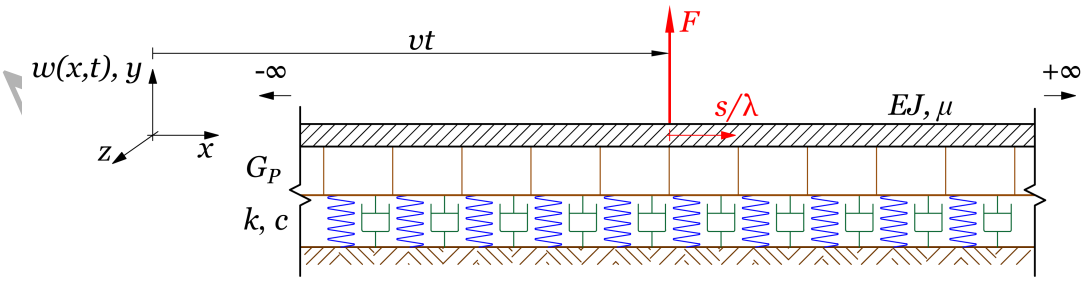

Figure 1: *Infinite Euler-Bernoulli elastic beam resting on a viscoelastic Pasternak foundation under a constant load F moving at constant velocity v along the beam.*

Then, Eq. (1), with $w(x,t)$ as in Eq. (2), may be rewritten with respect to a moving ref-

erence frame by introducing the following new non-dimensional real independent variable:

$$s = \lambda(x - vt); \qquad -\infty < s < +\infty; \qquad \lambda = \sqrt[4]{\frac{k}{4EJ}}; \tag{3}$$

Now, from the change of variables defined in Eq. (3), Eq. (2) reads

$$w(x,t) = w_0 \hat{w}(s); \tag{4}$$

and the chain rule of differentiation on Eq. (4), with s defined in Eq. (3), yields:

$$\begin{aligned} &\frac{\partial w(x,t)}{\partial x} = w_0 \lambda \frac{d\hat{w}(s)}{ds}, \qquad \frac{\partial^2 w(x,t)}{\partial x^2} = w_0 \lambda^2 \frac{d^2\hat{w}(s)}{ds^2}, \qquad \frac{\partial^4 w(x,t)}{\partial x^4} = w_0 \lambda^4 \frac{d^4\hat{w}(s)}{ds^4}; \\ &\frac{\partial w(x,t)}{\partial t} = -w_0 \lambda v \frac{d\hat{w}(s)}{ds}, \qquad \frac{\partial^2 w(x,t)}{\partial t^2} = w_0 \lambda^2 v^2 \frac{d^2\hat{w}(s)}{ds^2}. \end{aligned} \tag{5}$$

Substituting Eqs. (4) and (5) into Eq. (1), by taking into account the following characteristic property of the Dirac delta function (Buschman (1996) [47]):

$$\delta(x - vt) = \delta\left(\frac{s}{\lambda}\right) = \lambda\delta(s); \tag{6}$$

and rearranging all terms, leads to the following fourth-order Ordinary Differential Equation (ODE) in unknown steady-state non-dimensional displacement $\hat{w}(s)$:

$$\lambda^4 EJ \frac{d^4\hat{w}(s)}{ds^4} + \lambda^2(\mu v^2 - G_P)\frac{d^2\hat{w}(s)}{ds^2} - \lambda v c \frac{d\hat{w}(s)}{ds} + k\hat{w}(s) = \frac{\lambda F}{w_0}\delta(s). \tag{7}$$

The far-field boundary conditions of Eq. (7) dictates that at an infinite distance of moving load F, the beam deflection and its derivatives shall vanish:

$$\lim_{s\to\pm\infty} \hat{w}(s) = 0; \qquad \lim_{s\to\pm\infty} \frac{d^{(i)}\hat{w}(s)}{ds^i} = 0; \quad i = 1,2,3. \tag{8}$$

Hence, the advantage of transforming the equation of motion into a moving reference frame is that the steady-state solution becomes time invariant, i.e. it may be obtained as by solving a purely static problem, since the time variable has explicitly disappeared.

For the purposes of the forthcoming analytical developments and ensuing discussion, the following two non-dimensional real characteristic parameters α, β are introduced:

$$\alpha = \frac{\mu v^2 - G_P}{4\lambda^2 EJ} = \frac{v^2 - G_P/\mu}{\sqrt{4kEJ}/\mu} = \frac{v^2 - G_P/\mu}{v_{cr,W}^2} = \left(\frac{v}{v_{cr,W}}\right)^2 - g_P; \tag{9}$$

$$\beta = \frac{vc}{\lambda^3 EJ} = 8\,\frac{v}{v_{cr,W}}\,\zeta \geq 0; \tag{10}$$

where parameters

$$g_P = \frac{G_P}{\mu v_{cr,W}^2} = \frac{G_P}{\sqrt{4kEJ}}; \qquad \zeta = \frac{c}{2\sqrt{k\mu}}; \tag{11}$$

are non-dimensional Pasternak modulus of the foundation and damping ratio, respectively, and where

$$v_{cr,W} = 2\lambda\sqrt{\frac{EJ}{\mu}} = \sqrt[4]{\frac{4kEJ}{\mu^2}} \tag{12}$$

is the critical velocity of the moving load problem for a Winkler elastic foundation, i.e.

for G_P=0 (see e.g. Kenney (1954) [1]), as re-derived in the subsequent sections.

By virtue of such mathematical definitions of α and β, ODE Eq. (7) finally becomes

$$\frac{d^4\hat{w}(s)}{ds^4} + 4\alpha\frac{d^2\hat{w}(s)}{ds^2} - \beta\frac{d\hat{w}(s)}{ds} + 4\hat{w}(s) = \hat{F}\delta(s); \tag{13}$$

where $\hat{F}$=$F/(\lambda^3 EJw_0)$ is a non-dimensional amplitude of the moving load. Consequently, non-dimensional steady-state rotation, bending moment and shear force may be written in terms of the following relations:

$$\hat{\theta}(s) = \frac{\theta(x-vt)}{\theta_0} = \frac{1}{\theta_0}\frac{\partial w(x-vt)}{\partial x} = \frac{w_0\lambda}{\theta_0}\hat{w}'(s) = \hat{w}'(s); \tag{14a}$$

$$\hat{M}(s) = \frac{M(x-vt)}{M_0} = \frac{EJ}{M_0}\frac{\partial^2 w(x-vt)}{\partial x^2} = \frac{EJw_0\lambda^2}{M_0}\hat{w}''(s) = \hat{w}''(s); \tag{14b}$$

$$\hat{S}(s) = \frac{S(x-vt)}{S_0} = \frac{EJ}{S_0}\frac{\partial^3 w(x-vt)}{\partial x^3} = \frac{EJw_0\lambda^3}{S_0}\hat{w}'''(s) = \hat{w}'''(s); \tag{14c}$$

where

$$\theta_0 = \lambda w_0, \quad M_0 = \lambda^2 EJw_0, \quad S_0 = \lambda^3 EJw_0 \tag{15}$$

are chosen normalization factors for rotation, bending moment and shear force, respectively, so that $\hat{\theta}(s)$, $\hat{M}(s)$ and $\hat{S}(s)$ are directly expressed as the derivatives of unknown $\hat{w}(s)$. These will be set at a later stage.

Hence, the steady-state response is mathematically ruled by non-dimensional parameters α, β in Eqs. (9)-(10). The explicit analytical solution of Eq. (13) for some combinations of parameters α, β has been already conjectured in the literature, as earlier discussed in the Introduction. In the following sections, an accurate analysis of the general solution of Eq. (13), parametrized with respect to α, β, is developed, based on a rigorous derivation by a full Fourier transform approach, giving rise to a universal parametric representation.

2.2 Comments on the definition of the characteristic system parameters

Possible alternative definitions of the characteristic parameters that rule the analytical problem are feasible, based on the involved mechanical parameters (EJ, μ; k, G_P; c and v). In particular, by inspecting Eqs. (9)-(13) three main characteristic parameters appear to rule the beam-foundation system response (G_P, c and v, or their non-dimensional counterparts g_P, ζ and $v/v_{cr,W}$). The definition of α in Eq. (9) is consistent with that provided by Frýba (1972) [8] for a Winkler foundation (G_P=0), so that when G_P=0 the two definitions come up to coincide. Consequently, in order to achieve a differential equation containing two parameters only, parameter β in Eq. (10) has been defined as a function of both damping ratio and velocity ratio. This choice allows for a 2D representation of the solution domain in terms of two parameters α, β as done in Fig. 2, instead of a 3D representation on the above mentioned three physical parameters. The links between the former and the latter representation will be extensively illustrated in Fig. 7.

The present "mathematical" definition goes to the core of the analytical derivation, allowing for a true decoupling of effects in mathematical terms and referring to the source

differential equation (see final differential Eq. (13)). Thus, the above definitions constitute those leading to the simplest mathematical inspection, also for its physical implications, entailing the minimum number of parameters governing the system response. In fact, whatever choice of the parameters based on physical considerations will lead to three independent parameters governing the system (as shown in Eqs. (9)-(10)), thus making more intricate the a "priori" analysis of the possible evolutions of the system. In this sense, α, β shall be conceived as "mathematical" parameters, more than "physical" parameters, apt to rule the solution regimes in fourthcoming Fig. 2, and relevant outcoming solution characteristics, without impeding to appreciate physical implications in subsequent Fig. 7, as shown in the following sections.

3 Analytical steady-state solution by Fourier transform

The analytical solution of Eq. (13) with boundary conditions in Eq. (8) may be derived by the application of the Fourier integral transform, by starting from the following fundamental definitions:

$$\hat{W}(q) = \int_{-\infty}^{\infty} \hat{w}(s) e^{-\mathrm{i}sq}\, ds; \quad \hat{w}(s) = \frac{1}{2\pi} \int_{-\infty}^{\infty} \hat{W}(q) e^{\mathrm{i}sq}\, dq; \tag{16}$$

where s, $q \in \mathbb{R}$, i is the imaginary unit, $\hat{W}(q)$ is the Fourier transform of $\hat{w}(s)$, and, conversely, $\hat{w}(s)$ is the inverse Fourier transform of $\hat{W}(q)$. By applying Fourier transform (16) to Eq. (13), the expression of Fourier transform $\hat{W}(q)$ of $\hat{w}(s)$ may be represented as

$$\hat{W}(q) = \frac{\hat{F}}{q^4 - 4\alpha q^2 - \beta \mathrm{i} q + 4} = \frac{\hat{F}}{P(q)}; \tag{17}$$

where $P(q)$ is a fourth-order polynomial with complex coefficients, whose roots (system poles) take a main role in the subsequent derivation of $\hat{w}(s)$, since they represent the four isolated singularities of Fourier transform $\hat{W}(q)$.

The solution to Eq. (13) is then obtained by using inverse Fourier transform in Eq. (16), namely by inverting $\hat{W}(q)$ in Eq. (17):

$$\hat{w}(s) = \frac{\hat{F}}{2\pi} \int_{-\infty}^{+\infty} \frac{e^{\mathrm{i}sq}}{P(q)}\, dq \;=\; \frac{\hat{F}}{2\pi} \lim_{R \to +\infty} \int_{-R}^{R} \frac{e^{\mathrm{i}sq}}{P(q)}\, dq; \tag{18}$$

where R is an auxiliary real parameter, useful to perform the infinite integration through a limit process as $R \to \infty$. By applying a contour integration (Duffy (2004) [48]) technique, the integral in Eq. (18) may be expressed as

$$\lim_{R \to +\infty} \int_{-R}^{R} \frac{e^{\mathrm{i}sq}}{P(q)}\, dq \;=\; \lim_{R \to +\infty} \left(\oint_{\mathcal{C}} \frac{e^{\mathrm{i}sq}}{P(q)}\, dq - \int_{\mathcal{C}_R} \frac{e^{\mathrm{i}sq}}{P(q)}\, dq \right); \tag{19}$$

where $\mathcal{C}_R$ is a semicircle centered on the origin of the complex plane, either in the upper ($\mathcal{C}_R^+$) or lower ($\mathcal{C}_R^-$) half-plane and $\mathcal{C} = \mathcal{C}_R \cup (-R, R)$ is a closed curve, obtained by joining semicircle $\mathcal{C}_R$ and segment $(-R, R)$ on the real axis (see Fig. 3, later shown).

The integrals in Eq. (19) converge because the integrand is a *meromorphic* function (see e.g. Bak and Newman (2010) [49]). Since exponential $e^{\mathrm{i}sq}$ and fourth-order poly-

nomial $P(q)$ are *entire* functions, the poles of the integrand coincide with the roots of polynomial $P(q)$ in Eq. (17). Furthermore, when radius R finally goes to infinity, the integral along semicircle $\mathcal{C}_R$ in Eq. (19) vanishes. In fact, by the triangle inequality

$$|P(q)| \geq |q^4| - |-4\alpha q^2| - |-\beta \mathrm{i} q| - |4| = |q^4| - 4|\alpha q^2| - \beta\,|q| - 4; \tag{20}$$

absolute value of $P(q)$ is bounded from below and for $q \in \mathcal{C}_R$, i.e. for $|q|{=}R$, one gets

$$|P(q)|_{q\,\in\,\mathcal{C}_R} \geq R^4 \left(1 - \frac{4|\alpha|}{R^2} - \frac{\beta}{R^3} - \frac{4}{R^4}\right) = m_R. \tag{21}$$

As a result, the modulus of the integrand of the integral along semicircle $\mathcal{C}_R$ in Eq. (19) is bounded from above as follows:

$$\left|\frac{e^{\mathrm{i}sq}}{P(q)}\right| = \frac{\left|e^{\mathrm{i}s(a+ib)}\right|}{|P(q)|} = \frac{|e^{\mathrm{i}as}|\left|e^{-bs}\right|}{|P(q)|} = \frac{\left|e^{-bs}\right|}{|P(q)|} \leq \frac{1}{m_R} = \begin{cases} \text{for } q \in \mathcal{C}_R^+, & \text{if } s > 0; \\ \text{for } q \in \mathcal{C}_R^-, & \text{if } s < 0; \end{cases} \tag{22}$$

where a and b are the real and imaginary parts of q, respectively. Finally, the application of Jordan's lemma (see e.g. Duffy (2004) [48]) leads to the above stated vanishing result:

$$0 \leq \lim_{R\to+\infty}\left|\int_{\mathcal{C}_R} \frac{e^{\mathrm{i}sq}}{P(q)}\,dq\right| \leq \lim_{R\to+\infty} \frac{2R}{m_R}\int_0^{\pm\frac{\pi}{2}} e^{-2sR\theta/\pi} d\theta \leq \lim_{R\to+\infty} \frac{\pi}{m_R\,|s|}\Big(1 - e^{-|s|R}\Big) = 0. \tag{23}$$

Thus, by Cauchy's Residue Theorem (Bak and Newman (2010) [49]), one may write:

$$\begin{aligned} \hat{w}(s) &= \frac{\hat{F}}{2\pi} \lim_{R\to+\infty} \int_{-R}^{R} \frac{e^{\mathrm{i}sq}}{P(q)}\,dq = \frac{\hat{F}}{2\pi} \lim_{R\to+\infty} \oint_{\mathcal{C}} \frac{e^{\mathrm{i}sq}}{P(q)}\,dq = \\ &= \frac{\hat{F}}{2\pi}\Big(\pm 2\pi\mathrm{i} \sum_{k=1}^{n} \mathrm{Res}\Big\{\frac{e^{\mathrm{i}sq}}{P(q)}; q_k\Big\}\Big) = \pm\mathrm{i}\hat{F} \sum_{k=1}^{n} \mathrm{Res}\Big\{\frac{e^{\mathrm{i}sq}}{P(q)}; q_k\Big\}; \end{aligned} \tag{24}$$

where $\mathrm{Res}\{f; q_k\}$ denotes the residue of function f at pole q_k; n is the number of poles q_k placed inside closed curve $\mathcal{C}$, the plus or minus sign depending on whether the orientation of $\mathcal{C}$ is counterclockwise or clockwise, respectively. Specifically, the residue for a pole of order m may be evaluated according to the subsequent formula (Duffy (2004) [48]):

$$\mathrm{Res}\Big\{f(q); q_k\Big\} = \frac{1}{(m-1)!} \lim_{q\to q_k} \frac{d^{m-1}}{dq^{m-1}}\Big((q - q_k)^m\, f(q)\Big). \tag{25}$$

Since the integral in Eq. (24) depends on the location of poles q_k in the complex plane, it follows that characteristic system parameters α, β, contained in the expressions of such poles, imply different manifestations of the steady-state solution. The derivation of the expressions of the poles as a function of the system parameters and of the universal analytical solution in explicit form are carried out in the following section.

4 Inversion of the Fourier transform

4.1 Parametric location of the poles

Fourth-order polynomial $P(q)$ reported in Eq. (17) displays four zeros in the complex plane. To classify the nature of these roots as a function of real non-dimensional parameters α, β

it is more suitable to analyze real-coefficient polynomial (Achenbach and Sun (1965) [22]):

$$\hat{P}(r) = P(\mathrm{i}r) = r^4 + 4\alpha r^2 + \beta r + 4; \tag{26}$$

in complex variable $r{=}{-}iq$. Let Δ be the discriminant of $\hat{P}(r)$, i.e. the product of the squares of the differences of the roots of $\hat{P}(r){=}0$ (see e.g. Rees (1922) [50]).

Denoting by r_k the roots of $\hat{P}(r)$ and by r'_k the roots of the first-order derivative of $\hat{P}(r)$, namely $\hat{P}'(r)$, by virtue of a theorem reported by Rees (1922) [50] one has

$$\Delta(\alpha,\beta){=}\prod_{k=1}^{4}\prod_{j>k}(r_k-r_j)^2{=}4^4\prod_{k=1}^{4}\hat{P}(r'_k){=}16384\left(\alpha^2-1\right)^2-256\alpha\left(\alpha^2-9\right)\beta^2-27\beta^4; \tag{27}$$

where the final expression of $\Delta(\alpha,\beta)$ may be readily verified within Mathematica [51].

Four distinct roots	Case 1	$\Delta>0,\ \alpha<-1$	$r_1{=}b_1;\ \ r_2{=}b_2;$ $r_3{=}b_3;\ \ r_4{=}b_4;$	$q_1{=}b_1\mathrm{i};\ \ q_2{=}b_2\mathrm{i};$ $q_3{=}b_3\mathrm{i};\ \ q_4{=}b_4\mathrm{i};$
	Case 2	$\Delta<0,\ \forall\,\alpha$	$r_1{=}b_1;\ \ r_2{=}b_2;$ $r_3{=}b_3+a_3\mathrm{i};$ $r_4{=}b_3-a_3\mathrm{i};$	$q_1{=}b_1\mathrm{i};\ \ q_2{=}b_2\mathrm{i};$ $q_3{=}-a_3+b_3\mathrm{i};$ $q_4{=}a_3+b_3\mathrm{i};$
	Case 3	$\Delta>0,\ \alpha>-1$	$r_1{=}b_1+a_1\mathrm{i};$ $r_2{=}b_1-a_1\mathrm{i};$ $r_3{=}b_3+a_3\mathrm{i};$ $r_4{=}b_3-a_3\mathrm{i};$	$q_1{=}-a_1+b_1\mathrm{i};$ $q_2{=}a_1+b_1\mathrm{i};$ $q_3{=}-a_3+b_3\mathrm{i};$ $q_4{=}a_3+b_3\mathrm{i};$
At least two coincident roots	Case 4	$\Delta{=}0,\ \alpha<-1$	$r_1{=}b_1;\ \ r_2{=}b_2;$ $r_3{=}r_4=b_3;$	$q_1{=}b_1\mathrm{i};\ \ q_2{=}b_2\mathrm{i};$ $q_3{=}q_4{=}b_3\mathrm{i};$
	Case 5	$\Delta{=}0,\ \alpha>-1$	$r_1{=}b_1;\ \ r_2{=}b_1;$ $r_3{=}b_3+a_3\mathrm{i};$ $r_4{=}b_3-a_3\mathrm{i};$	$q_1{=}q_2{=}b_1\mathrm{i};$ $q_3{=}-a_3+b_3\mathrm{i};$ $q_4{=}a_3+b_3\mathrm{i};$
	Case 6	$\beta{=}0,\ \alpha\geq 1$ $(\Delta\geq 0)$	$r_1{=}a_1\mathrm{i};\ \ r_2{=}-a_1\mathrm{i};$ $r_3{=}a_3\mathrm{i};\ \ r_4{=}-a_3\mathrm{i};$	$q_1{=}-a_1;\ \ q_2{=}a_1;$ $q_3{=}-a_3;\ \ q_4{=}a_3;$

Table 1: *Classification of the nature of roots r_k of $\hat{P}(r)$ and q_k of $P(q)$ as a function of system parameters α, β; real-valued a_i, b_i define real and imaginary parts of the roots.*

The sign of $\Delta(\alpha,\beta)$ is crucial to determine the nature of the poles (Dickson (1914) [52]). In fact, the four roots of $\hat{P}(r){=}0$ with real coefficients and discriminant $\Delta(\alpha,\beta)$ take the form reported in Table 1. Consequently, by multiplying roots r_k by imaginary unit i, the form of roots q_k of denominator $P(q)$ are characterized, also listed in Table 1. A graphical representation of the nature of roots q_k of $P(q)$ as a function of characteristic parameters α and β is depicted in Fig. 2, where a subdivision of the parametric space into different subdomains is pointed out. Such a partition is fundamental for characterizing the behavior of the beam-foundation response, as it will be outlined in following Section 5.

4.2 Parametric expression of the poles

As exposed in Section 3, the key feature for the inversion of the Fourier transform in Eq. (16) is the characterization of the nature of poles q_k as a function of system parameters α, β. In this section, exact symbolic expressions of these roots are provided.

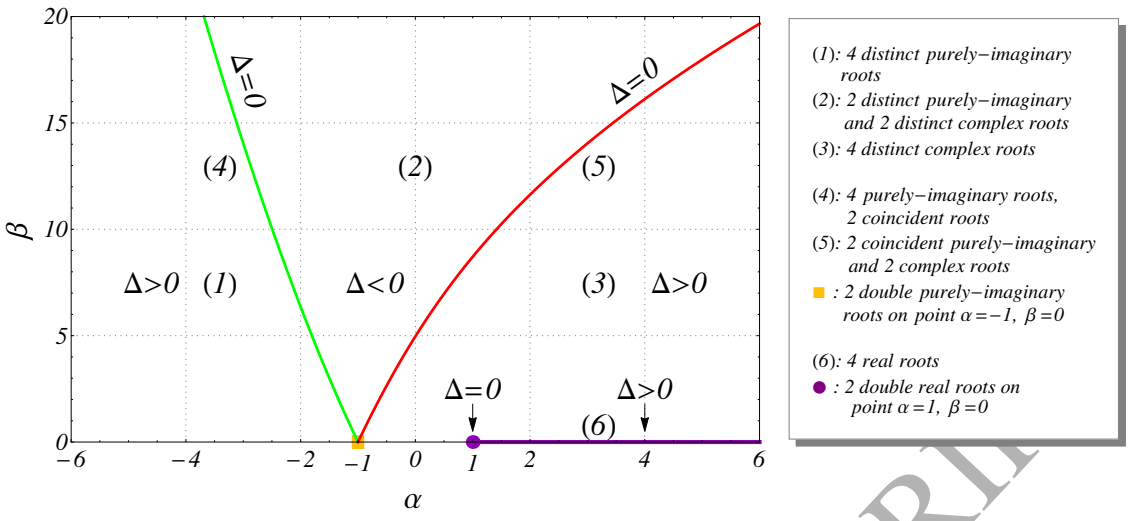

Figure 2: *Graphical representation of the solution regions in the domain of system parameters α, β with the same type of q_k roots.*

By virtue of the analysis in Section 4.1, roots q_k take the subsequent general form:

$$q_1 = -a_1 + \mathrm{i}b_1; \quad q_2 = a_1 + \mathrm{i}b_2; \quad q_3 = -a_3 + \mathrm{i}b_3; \quad q_4 = a_3 + \mathrm{i}b_4; \tag{28}$$

where a_1, a_3 and b_1, b_2, b_3, b_4 are six real coefficients, labeling the real and imaginary parts of roots q_k, respectively. In order for q_k to be a root of polynomial $P(q)$, above-defined coefficients a_i and b_i have to be related to the coefficients of $P(q)$.

Such relationships may be obtained by Vieta's formulas (see e.g. Vinberg (2003) [53]), relating the coefficients of polynomial $P(q)$ to sums and products of its roots, as follows:

$$\sum_{1\le i\le 4} q_i = 0; \quad \sum_{1\le i<j\le 4} q_i q_j = -4\alpha; \quad \sum_{1\le i<j<k\le 4} q_i q_j q_k = -\beta\mathrm{i}; \quad \sum_{1\le i<j<k<l\le 4} q_i q_j q_k q_l = 4. \tag{29}$$

By using other auxiliary real constants A_i, defined as:

$$A_1 = a_1^2 + b_1 b_2; \quad A_2 = b_1 + b_2; \quad A_3 = a_3^2 + b_3 b_4; \quad A_4 = b_3 + b_4; \tag{30}$$

and according to Table 1, which implies one of the following three occurrences:

$$a_1 = a_3 = 0 \quad \text{or} \quad a_1 = 0 \text{ and } b_3 = b_4 \quad \text{or} \quad a_1, a_3 \neq 0 \text{ and } b_1 = b_2,\, b_3 = b_4; \tag{31}$$

the system of Eqs. (29) becomes:

$$A_2 + A_4 = 0; \quad A_1 + A_3 + A_2 A_4 = 4\alpha; \quad (A_1 A_4 + A_2 A_3)\mathrm{i} = -\beta\mathrm{i}; \quad A_1 A_3 = 4. \tag{32}$$

The solution of the nonlinear system of Eqs. (32) may be expressed as:

$$A_1 = \frac{A_4^2}{2} + 2\alpha - \frac{\beta}{2A_4}; \qquad A_2 = -A_4; \qquad A_3 = \frac{A_4^2}{2} + 2\alpha + \frac{\beta}{2A_4}; \tag{33}$$

where coefficient A_4 comes by solving the following sixth-order polynomial equation:

$$A_4^6 - 8\alpha A_4^4 + 16(\alpha^2 - 1)A_4^2 - \beta^2 = 0; \tag{34}$$

which may be further recast into a third-order polynomial equation:

$$t^3 - 8\alpha t^2 + 16(\alpha^2 - 1)t - \beta^2 = 0; \tag{35}$$

by defining auxiliary variable $t{=}A_4^2$. Since, by definition, A_4 in Eqs. (30) is a real number, only positive values of t have to be taken into account amongst the three solutions of Eq. (35). The discriminant of the cubic polynomial in Eq. (35), evaluated in accordance to Dickson (1914) [52], is exactly the quantity Δ reported in Eq. (27), expressing the discriminant of the quartic polynomial in Eq. (26). Following a theorem reported by Dickson (1914) [52] a cubic polynomial equation has always at least a real root, independently from the sign of its discriminant; furthermore, at least one positive root must exist since constant term $-\beta^2$ in Eq. (35) is negative.

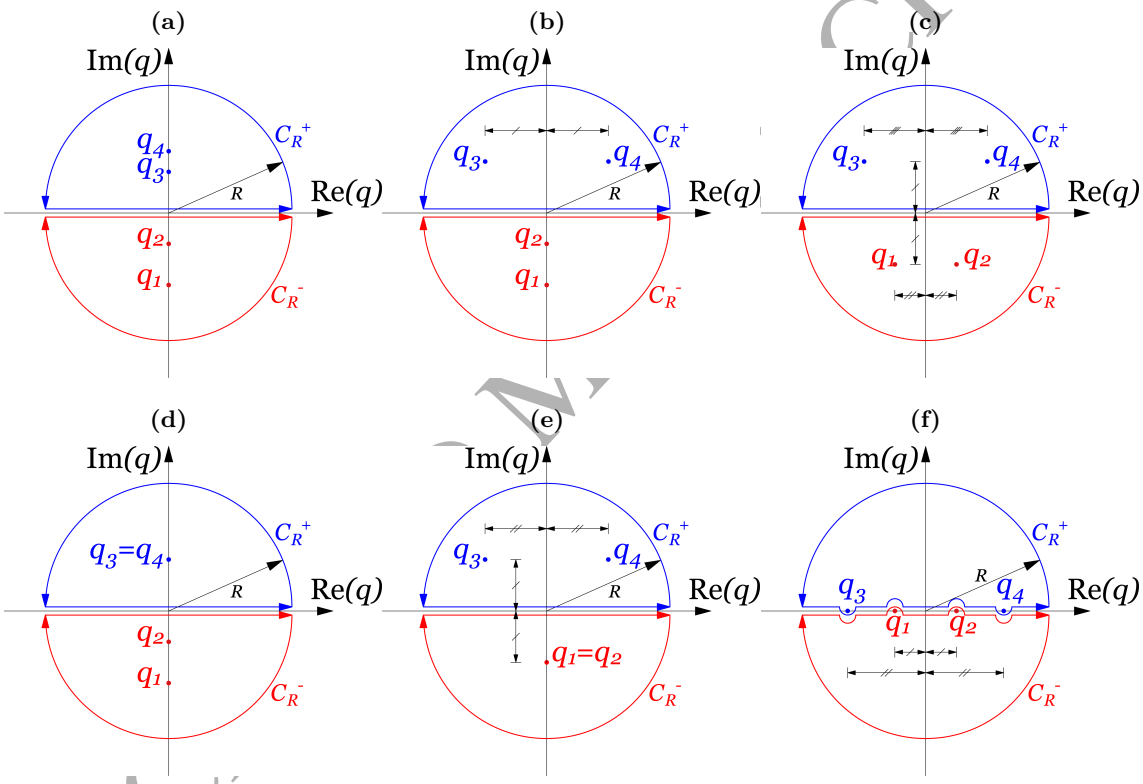

Figure 3: *Poles q_k in the complex plane (Case 1 (**a**); Case 2 (**b**); Case 3 (**c**); Case 4 (**d**); Case 5 (**e**); Case 6 (**f**)).*

The choice of the sign of $A_4{=}\pm\sqrt{t}$ is arbitrary and not significant towards the derivation of the solution, since it induces only an exchange of values between roots q_1, q_2 and q_3, q_4. In the following, a plus sign is considered; thus, A_4 is a non-negative real number. The explicit expression of quantity $A_4{=}\sqrt{t}$ has been derived within Mathematica [51], where Cardan's formula is implemented by a built-in function, and takes the following final form:

$$A_4(\alpha,\beta) = \frac{1}{\sqrt{3}}\sqrt{\frac{16(\alpha^2+3)}{f(\alpha,\beta)} + f(\alpha,\beta) - 8\alpha}; \tag{36a}$$

$$f(\alpha,\beta)=\sqrt[3]{\frac{27}{2}\beta^2+64\alpha(\alpha^2-9)+3\frac{\sqrt{3}}{2}\sqrt{-\Delta(\alpha,\beta)}}. \tag{36b}$$

It may be shown that expressions (36a)-(36b) always lead to a real non-negative coefficient A_4. Then, the final expressions of unknown coefficients a_1, a_3, b_1, b_2, b_3, b_4 become:

$$a_1=\begin{cases}0 & \text{if } 4A_1-A_4^2=A_4^2+8\alpha-2\beta/A_4\le 0;\\ \frac{1}{2}\sqrt{4A_1-A_4^2} & \text{otherwise } (\Delta>0,\ \alpha\le -1);\end{cases} \tag{37a}$$

$$a_3=\begin{cases}0 & \text{if } 4A_3-A_4^2=A_4^2+8\alpha+2\beta/A_4\le 0;\\ \frac{1}{2}\sqrt{4A_3-A_4^2} & \text{otherwise } (\Delta<0;\ \Delta>0,\ \alpha\ge -1);\end{cases} \tag{37b}$$

$$b_{1,2}=-\frac{1}{2}\Big(A_4\mp\sqrt{4a_1^2-4A_1+A_4^2}\Big);\quad b_{3,4}=\frac{1}{2}\Big(A_4\mp\sqrt{4a_3^2-4A_3+A_4^2}\Big); \tag{37c}$$

where the choice among the two alternatives for a_1 and a_3 in Eqs. (37a) and (37b), respectively, depends on the sign of the term under square root. Since $A_4=\sqrt{t}\ge 0$, by definition, from Eqs. (28) and Eqs. (37) it results that roots q_1, q_2 are always placed in the lower half-plane of the complex plane, while roots q_3, q_4 are located in the upper half-plane. The possible loci of the roots in the complex plane arising from the above analysis are represented in Fig. 3, where contour paths explained earlier in Section 3 are also depicted.

Notice that the possibility of a vanishing A_4 represents a singular case in the above derivation, meaning that roots q_k cannot be represented by Eqs. (37). This occurrence corresponds to the appearance of four real roots, as it will be shown in following Section 4.4. The derivation of the final analytical solution by contour integration now follows.

4.3 Derivation of the universal analytical solution

According to the graphical representation of the poles (Table 1) provided in Figs. 3a-3c and given Eq. (25), the residues of the integrand in Eq. (24) for non-coincident poles (poles of first-order) are computed as:

$$\mathrm{Res}\Big\{\frac{e^{\mathrm{i}sq}}{P(q)};q_k\Big\}=\frac{e^{\mathrm{i}sq_k}}{P'(q_k)}=e^{\mathrm{i}sq_k}\prod_{j=1,\,j\neq k}^{4}(q_k-q_j)^{-1}; \tag{38}$$

and then the final non-dimensional deflection solution becomes

$$\hat{w}(s)=\hat{w}^-(s)=-\mathrm{i}\hat{F}\,\frac{(q_2-q_3)(q_2-q_4)e^{\mathrm{i}q_1s}-(q_1-q_3)(q_1-q_4)e^{\mathrm{i}q_2s}}{(q_1-q_2)(q_1-q_3)(q_1-q_4)(q_2-q_3)(q_2-q_4)},\quad \text{for } s\le 0; \tag{39a}$$

$$\hat{w}(s)=\hat{w}^+(s)=\mathrm{i}\hat{F}\,\frac{(q_3-q_1)(q_3-q_2)e^{\mathrm{i}q_3s}-(q_4-q_1)(q_4-q_2)e^{\mathrm{i}q_4s}}{(q_3-q_4)(q_3-q_1)(q_3-q_2)(q_4-q_1)(q_4-q_2)},\quad \text{for } s\ge 0. \tag{39b}$$

By further rearranging terms in Eq. (39), the non-dimensional deflection solution may be written as follows:

$$\hat{w}(s)=\hat{w}^-(s)=\frac{\hat{F}}{B_5}\,\frac{B_2e^{-(a_1\mathrm{i}+b_1)s}-B_1e^{(a_1\mathrm{i}-b_2)s}}{B_1\,B_2},\quad \text{for } s\le 0; \tag{40a}$$

$$\hat{w}(s)=\hat{w}^+(s)=\frac{\hat{F}}{B_6}\,\frac{B_4e^{-(a_3\mathrm{i}+b_3)s}-B_3e^{(a_3\mathrm{i}-b_4)s}}{B_3\,B_4},\quad \text{for } s\ge 0; \tag{40b}$$

where coefficients B_i, introduced to further simplify the notation, are defined as

$$B_1 = -(q_1 - q_3)(q_1 - q_4) = \frac{\beta}{A_4} + A_4^2 - A_4 B_5; \tag{41a}$$

$$B_2 = -(q_2 - q_3)(q_2 - q_4) = \frac{\beta}{A_4} + A_4^2 + A_4 B_5; \tag{41b}$$

$$B_3 = (q_3 - q_1)(q_3 - q_2) = \frac{\beta}{A_4} - A_4^2 - A_4 B_6; \tag{41c}$$

$$B_4 = (q_4 - q_1)(q_4 - q_2) = \frac{\beta}{A_4} - A_4^2 + A_4 B_6; \tag{41d}$$

$$B_5 = -(q_1 - q_2)\mathrm{i} = \mathrm{i}\sqrt{A_4^2 + 8\alpha - 2\beta/A_4}; \tag{41e}$$

$$B_6 = -(q_3 - q_4)\mathrm{i} = \mathrm{i}\sqrt{A_4^2 + 8\alpha + 2\beta/A_4}; \tag{41f}$$

and the coefficients involved in the exponential functions have been written as:

$$a_1\mathrm{i} + b_1 = -\frac{A_4 - B_5}{2};\quad a_1\mathrm{i} - b_2 = \frac{A_4 + B_5}{2};\quad a_3\mathrm{i} + b_3 = \frac{A_4 + B_6}{2};\quad a_3\mathrm{i} - b_4 = -\frac{A_4 - B_6}{2}; \tag{42}$$

where coefficient A_4 has been defined in Eqs. (36). From the expressions of the solution in Eqs. (40), the steady-state solution turns out proportional to $\hat{F}$ (thus to the moving load amplitude F), as it was expected from the linearity of the source differential equation.

By combining Eqs. (40)-(41)-(42), the *final universal non-dimensional solution of the steady-state vibration of the infinite beam* in explicit form is given by

$$\hat{w}(s) = \hat{w}^-(s) = \frac{\hat{F}}{B_5}\,\frac{B_2 e^{(A_4 - B_5)s/2} - B_1 e^{(A_4 + B_5)s/2}}{B_1\, B_2}, \qquad \text{for } s \le 0; \tag{43a}$$

$$\hat{w}(s) = \hat{w}^+(s) = \frac{\hat{F}}{B_6}\,\frac{B_4 e^{-(A_4 + B_6)s/2} - B_3 e^{-(A_4 - B_6)s/2}}{B_3\, B_4}, \qquad \text{for } s \ge 0; \tag{43b}$$

Notice that when coefficient B_5 becomes purely imaginary, that is when $\Delta{>}0$ and $\alpha{\ge}{-}1$, the half of its absolute value ($|B_5|/2$) represents the frequency of oscillation of the wave propagating backward with respect to the moving load ($\hat{w}^-(s)$). Instead, when B_5 is real, no propagation of waves appears behind the moving load, but the response is described by the difference of two exponentially decaying functions (evanescent wave). Accordingly, the same features characterize the response of the part of the beam placed on the right of the moving load ($\hat{w}^+(s)$), in terms of coefficient B_6; in fact, if B_6 becomes purely imaginary ($\Delta{<}0$ or $\Delta{>}0$ and $\alpha{\ge}{-}1$), $|B_6|/2$ represents the frequency of oscillation of the wave propagating forward from the moving load.

The final achieved analytical representation of the steady-state response is resumed in synoptic form in the sketch provided in Fig. 4, where all the necessary ingredients are included. The representation and interpretation of such achieved analytical steady-state solution is going to be presented and discussed in detail in Section 5, but, first, singular cases of the dynamic response are further commented in Section 4.4 below.

Notice that, despite for these singular cases, the achieved analytical solution provides a

SYNOPSIS OF THE STEADY-STATE ANALYTICAL SOLUTION

Definitions

- $s = \lambda(x - vt)$; $\quad \lambda = \sqrt[4]{\dfrac{k}{4EJ}}$;
- $w(s) = w_0 \hat{w}(s)$; $\quad \hat{F} = \dfrac{F}{\lambda^3 EJ w_0}$;
- $\alpha = \dfrac{v^2 - G_P/\mu}{v_{cr,W}^2}$; $\quad \beta = \dfrac{vc}{\lambda^3 EJ}$; $\quad v_{cr,W} = \sqrt[4]{\dfrac{4kEJ}{\mu^2}}$;

Governing differential equation and boundary conditions

- $\hat{w}^{(4)}(s) + 4\alpha\hat{w}^{(2)}(s) - \beta\hat{w}^{(1)}(s) + 4\hat{w}(s) = \hat{F}\delta(s), \quad -\infty < s < \infty$;
- $\lim\limits_{s\to\pm\infty} \hat{w}(s) = 0$; $\quad \lim\limits_{s\to\pm\infty} \hat{w}^{(1)}(s) = 0$;

General solution ($\Delta \neq 0$)

- $\hat{w}(s) = \hat{w}^-(s) = \dfrac{\hat{F}}{B_5} \dfrac{B_2 e^{(A_4 - B_5)s/2} - B_1 e^{(A_4 + B_5)s/2}}{B_1 B_2}$, *for* $s \leq 0$;
- $\hat{w}(s) = \hat{w}^+(s) = \dfrac{\hat{F}}{B_6} \dfrac{B_4 e^{-(A_4 + B_6)s/2} - B_3 e^{-(A_4 - B_6)s/2}}{B_3 B_4}$, *for* $s \geq 0$;

where:

- $B_1 = \dfrac{\beta}{A_4} + A_4^2 - A_4 B_5$; $\quad B_2 = \dfrac{\beta}{A_4} + A_4^2 + A_4 B_5$; $\quad B_5 = i\sqrt{A_4^2 + 8\alpha - 2\beta/A_4}$;
- $B_3 = \dfrac{\beta}{A_4} - A_4^2 - A_4 B_6$; $\quad B_4 = \dfrac{\beta}{A_4} - A_4^2 + A_4 B_6$; $\quad B_6 = i\sqrt{A_4^2 + 8\alpha + 2\beta/A_4}$;
- $A_4(\alpha, \beta) = \dfrac{1}{\sqrt{3}} \sqrt{\dfrac{16(\alpha^2 + 3)}{f(\alpha, \beta)} + f(\alpha, \beta) - 8\alpha}$;
  - $f(\alpha, \beta) = \sqrt[3]{\dfrac{27}{2}\beta^2 + 64\,\alpha(\alpha^2 - 9) + 3\dfrac{\sqrt{3}}{2}\sqrt{-\Delta(\alpha, \beta)}}$;
    - $\Delta(\alpha, \beta) = 16384\left(\alpha^2 - 1\right)^2 - 256\,\alpha\left(\alpha^2 - 9\right)\beta^2 - 27\beta^4$

Figure 4: *Synoptic chart of the universal steady-state analytical solution of the beam-Pasternak foundation system. Corresponding responses are plotted in Figs. 8-11.*

universal representation for all the regular solution instances, namely Cases (1), (2) and (3) with $\Delta \neq 0$ in Fig. 2, starting from the general form of the roots in Eq. (28). This is a main achievement of the present derivation.

From the final expression of the solution in Eqs. (43), it is straightforward to derive the normalized response characteristics (Eqs. (14)) at the point underneath the load (s=0), which take the following analytical representations:

$$\hat{w}(0) = \hat{F}\frac{B_2 - B_1}{B_1 B_2 B_5} = 2\hat{F}\frac{A_4}{B_1 B_2} = \hat{F}\frac{2A_4^3}{2A_4^6 + 8\alpha A_4^4 + \beta^2}; \tag{44a}$$

$$\hat{\theta}(0) = \hat{F}\,\frac{B_2(A_4-B_5)-B_1(A_4+B_5)}{2B_1B_2B_5} = \hat{F}\,\frac{A_4\beta}{2A_4^6+8\alpha A_4^4+\beta^2}; \tag{44b}$$

$$\hat{M}(0) = \hat{F}\,\frac{B_2(A_4-B_5)^2-B_1(A_4+B_5)^2}{4B_1B_2B_5} = \hat{F}\,\frac{-A_4^3\left(A_4^2+4\alpha\right)}{2A_4^6+8\alpha A_4^4+\beta^2}; \tag{44c}$$

$$\hat{S}(0^-) = \hat{F}\,\frac{B_2(A_4-B_5)^3-B_1(A_4+B_5)^3}{8B_1B_2B_5} = \frac{\hat{F}}{2}\left(\frac{A_4\beta(A_4^2+4\alpha)}{2A_4^6+8\alpha A_4^4+\beta^2}-1\right); \tag{44d}$$

$$\hat{S}(0^+) = \hat{F}\,\frac{B_3(A_4-B_6)^3-B_4(A_4+B_6)^3}{8B_3B_4B_6} = \frac{\hat{F}}{2}\left(\frac{A_4\beta(A_4^2+4\alpha)}{2A_4^6+8\alpha A_4^4+\beta^2}+1\right). \tag{44e}$$

which will be used in the later illustrations in Section 5.

4.4 Singular cases

The analytical solution in Eq. (43), provided in parametric form, is able to represent the response of the system everywhere in the domain of system parameters α and β, except for two singular situations (Cases (4)-(5) and Case (6) in Table 1 and Figs. 2-3):

- the first considered singular instance corresponds to Case (6), namely $\Delta{\geq}0$, with $\alpha{\geq}1$ and $\beta{=}0$, and is referred to the occurence in which coefficient A_4 becomes null (situation which also includes the case when coefficients B_i, $i{=}1,2,3,4$, may vanish);
- the second considered singular situation occurs when B_5 or B_6, which appear in the denominators of $\hat{w}^-(s)$ and $\hat{w}^+(s)$, respectively, become null; from their definitions given in Eqs. (41e) and (41f), B_5 or B_6 may become null if and only if poles q_1, q_2 and q_3, q_4 come to coincide, respectively, that is if $\Delta{=}0$ (Cases (4)-(5)).

For these two specific occurrences, treated in the following, the solution has to be derived independently from Eq. (43), leading to the derivation of the *critical velocity* and of the *critical damping* for a beam-Pasternak foundation system, respectively.

4.4.1 Undamped supercritical stage and critical velocity

As earlier mentioned in Section 4, the singular case of $A_4(\alpha,\beta)$ becoming null must be separately treated from the above derived general formulation. As it may be checked from Eqs. (36), this situation occurs for $\beta{=}0$ and $\alpha{\geq}1$, corresponding to Case (6) in Table 1 and Figs. 2-3. The resulting expressions of the four real roots of $P(q)$ become:

$$q_1 = -a_1 = -\sqrt{2}\sqrt{\alpha-\sqrt{\alpha^2-1}}; \quad q_2 = a_1 = \sqrt{2}\sqrt{\alpha-\sqrt{\alpha^2-1}}; \tag{45a}$$

$$q_3 = -a_3 = -\sqrt{2}\sqrt{\alpha+\sqrt{\alpha^2-1}}; \quad q_4 = a_3 = \sqrt{2}\sqrt{\alpha+\sqrt{\alpha^2-1}}. \tag{45b}$$

In deriving the non-dimensional solution of Eq. (13) in case of real roots, the first step is to avoid the singularity on the integration path by deforming the contour in a small, semicircular path (indentation) either above or below the poles (in the sense of Cauchy principal value, see Duffy (2004) [48]). Such an indentation will include or exclude a singularity from the contour of integration, depending on whether the overall closure of the contour is above or below the real axis. The indentations of the paths represented in

Fig. 3f are determined in continuity with the representation in Fig. 3c, i.e. by including the same poles, having now null imaginary parts (β=0), within the corresponding contours.

Then, the non-dimensional solution of Eq. (13) for this singular case is obtained as:

$$\hat{w}^{-}(s) = -\mathrm{i}\hat{F}\,\frac{e^{-\mathrm{i}a_1 s} - e^{\mathrm{i}a_1 s}}{-2a_1(a_1^2 - a_3^2)} = \hat{F}\,\frac{\sin(a_1 s)}{a_1(a_1^2 - a_3^2)}, \quad \text{for } s \le 0; \tag{46a}$$

$$\hat{w}^{+}(s) = \mathrm{i}\hat{F}\,\frac{e^{-\mathrm{i}a_3 s} - e^{\mathrm{i}a_3 s}}{-2a_3(a_3^2 - a_1^2)} = \hat{F}\,\frac{\sin(a_3 s)}{a_3(a_1^2 - a_3^2)}, \quad \text{for } s \ge 0. \tag{46b}$$

Eqs. (46) show that resonance occurs as α approaches 1 (a_1=a_3=$\sqrt{2}$, double pole on the real axis), in the sense that the amplitude of the traveling waves, which increases without bound, can no longer be defined. The nonexistence of the solution may be also justified by the nonexistence of the integral in Eq. (18) for α=1:

$$\hat{w}(s) = \frac{\hat{F}}{2\pi}\int_{-\infty}^{+\infty}\frac{e^{\mathrm{i}sq}}{P(q)}\,dq = \frac{\hat{F}}{2\pi}\int_{-\infty}^{+\infty}\frac{e^{\mathrm{i}sq}}{(q-\sqrt{2})^2(q+\sqrt{2})^2}\,dq\,; \tag{47}$$

even in the sense of Cauchy principal value, as it was shown by Buta and Jones (1964) [23] and by Achenbach and Sun (1965) [22].

By inverting Eq. (9), with α=1, the velocity of the moving load at which such instability occurs, i.e. the critical velocity for a beam-Pasternak foundation system, is obtained as

$$v_{cr,P} = \sqrt{v_{cr,W}^2 + \frac{G_P}{\mu}} = v_{cr,W}\sqrt{1+g_P} = v_{cr,W}\sqrt{1+\frac{1}{2}\sqrt{\frac{G_P}{k}}\sqrt{\frac{G_P}{EJ}}}; \tag{48}$$

where g_P and $v_{cr,W}$ were defined in Eq. (11) and Eq. (12), respectively. The expression of the critical velocity in Eq. (48) is the same as that reported by Kerr (1972) [27], by Mallik (2006) [39] and by Basu and Kameswara Rao (2013) [40].

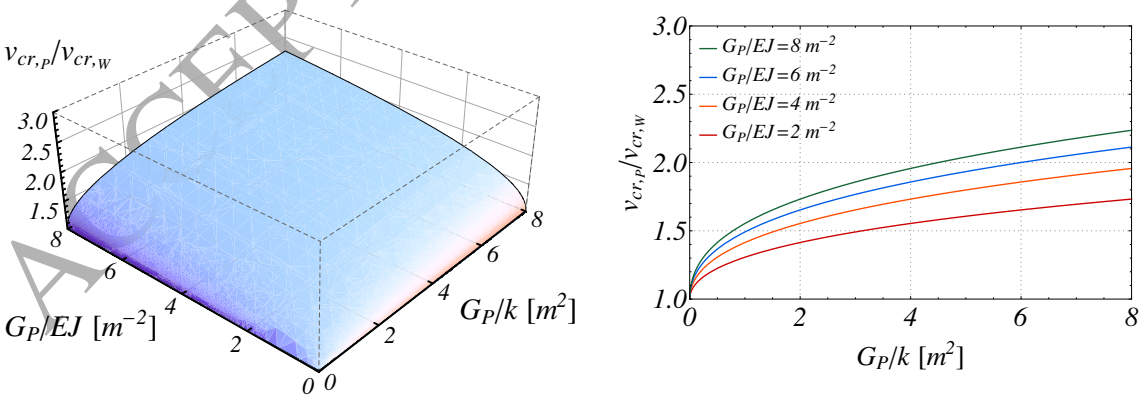

Figure 5: *Representation of Pasternak/Winkler critical velocity ratio as a function of foundation moduli ratio G_P/k and Pasternak modulus/bending stiffness ratio G_P/EJ.*

Fig. 5 shows Pasternak/Winkler critical velocity ratio $v_{cr,P}/v_{cr,W}$, as a function of the stiffness parameters of the beam-foundation system according to Eq. (48). Velocity ra-

tio $v_{cr,P}/v_{cr,W}$ depends on the ratios between Pasternak modulus G_P and both Winkler foundation coefficient k and beam bending stiffness EJ, respectively. Given the high initial steepness of the curves in these plots, the velocity ratio grows rather quickly, even for small values of coefficient ratio G_P/k, meaning that the threshold of the critical velocity may be raised by considering even only a little amount of shear interaction between the foundation springs. Such shear interaction leads to a beneficial effect in structural terms by increasing the critical velocity, since the whole model stiffness is increased.

For $\alpha>1$ and $\beta=0$, both waves are described by finite-amplitude undamped harmonic oscillations, violating the far-field conditions in Eq. (8), which state a zero response at $\pm\infty$. Hence, the undamped response of the beam-foundation system at the supercritical velocities cannot be evaluated by the present approach, namely the beam never attains a steady-state condition for the ideal undamped case. Different is the case when there is an even slight amount of viscous damping and the moving load velocity is not null ($v\neq0$). In fact, since the system is able to dissipate energy by virtue of its infinite extension, a solution that complies with the far-field conditions always exists.

4.4.2 Critical damping

By looking at the classification reported in Table 1, the situation for which two poles come to coincide or, in other words a pole of second-order appears, is determined by the discriminant $\Delta(\alpha,\beta)$ in Eq. (27) becoming zero. Such occurrence may appear twice, except for the case discussed in the previous subsection, either for $q_1=q_2$, i.e. for $B_5=0$ (Case (5), $\Delta=0$ and $\alpha>-1$, red curve in Fig. 2), or for $q_3=q_4$, i.e. for $B_6=0$ (Case (4), $\Delta=0$ and $\alpha<-1$, green curve in Fig. 2).

Such two cases describe the transition from an evanescent wave to a propagating leftward wave ($\hat{w}^-(s)$), Case (5), or to a propagating rightward wave ($\hat{w}^+(s)$), Case (4), respectively. Indeed, since these special responses are characterized by a zero frequency of oscillation, their wavelength becomes infinite. This condition arises in the case of *critical damping* (Basu and Kameswara Rao (2013) [40]).

The critical damping condition may be determined from the expression of $\Delta(\alpha,\beta)$ in Eq. (27) by solving the polynomial equation $\Delta(\alpha,\beta)=0$ (biquadratic in β) with respect to β, which, by considering only real and non-negative values of β in Eq. (10), gives

$$\beta_{cr,P}=\frac{8\sqrt{2}}{3\sqrt{3}}\sqrt{\alpha(9-\alpha^2)+\sqrt{(\alpha^2+3)^3}}; \tag{49}$$

and which, rewritten in terms of the physical parameters of the system, provides the expression of the critical damping coefficient for a Pasternak elastic foundation:

$$c_{cr,P}=2\sqrt{k\mu}\cdot\frac{\sqrt{2}}{3\sqrt{3}}\frac{v_{cr,W}}{v}\sqrt{\left(\frac{v^2-G_P/\mu}{v_{cr,W}^2}\right)\left(9-\left(\frac{v^2-G_P/\mu}{v_{cr,W}^2}\right)^2\right)+\left(\left(\frac{v^2-G_P/\mu}{v_{cr,W}^2}\right)^2+3\right)^{\frac{3}{2}}}; \tag{50}$$

where $2\sqrt{k\mu}$ represents a reference critical damping coefficient of a classical spring-mass system (see Eq. (11)).

As already noticed by Frýba (1972) [8] for a Winkler-type foundation (G_P=0), Eq. (50) points out that, in addition to the mechanical parameters of the beam-Pasternak foundation system, the critical damping coefficient depends also upon moving load velocity v. Notice that, for G_P=0, the value of the critical damping coefficient of a Winkler foundation is recovered (see Fryba (1972) [8]):

$$c_{cr,W} = 2\sqrt{k\mu}\cdot\frac{\sqrt{2}}{3\sqrt{3}}\sqrt{\left(9-\left(\frac{v}{v_{cr,W}}\right)^4\right)+\left(\frac{v_{cr,W}}{v}\right)^2\left(\left(\frac{v}{v_{cr,W}}\right)^4+3\right)^{\frac{3}{2}}}. \tag{51}$$

Furthermore, for a Winkler foundation (G_P=0, thus $\alpha\geq 0$) or for a Pasternak elastic foundation subjected to the condition $G_P>\sqrt{4kEJ}$ (equivalent to $\alpha>-1$), given a certain damping coefficient c, there exists only one value of moving load velocity for which such value of damping becomes critical; this corresponds to a leftward beam response ($s<0$) characterized by a null frequency (B_5=0) and a corresponding infinite wavelength. Within such a situation, by applying Eq. (25), the residue of the integrand in Eq. (24) for coincident poles (poles of second-order) can be computed as ($j\neq k\neq l$):

$$\mathrm{Res}\left\{\frac{e^{\mathrm{i}sq}}{(q-q_j)(q-q_k)(q-q_l)^2};q_l\right\}=\frac{q_j+q_k-2q_l+(q_j-q_l)(q_k-q_l)\mathrm{i}s}{(q_l-q_j)^2(q_l-q_k)^2}\,e^{\mathrm{i}sq_l}. \tag{52}$$

According to the graphical representation of the poles provided in Fig. 3d and to Eq. (52), the critically damped solution for this singular case becomes for $s\leq 0$:

$$\hat{w}^-_{\beta_{cr}}(s)=-\mathrm{i}\hat{F}\,\frac{q_3+q_4-2q_1+(q_3-q_1)(q_4-q_1))\mathrm{i}s}{(q_3-q_1)^2(q_4-q_1)^2}\,e^{\mathrm{i}sq_1},\quad \text{for } s\leq 0; \tag{53}$$

and, by a further manipulation:

$$\boxed{\hat{w}^-_{\beta_{cr}}(s)=\hat{F}\,\frac{2A_4-B_1s}{B_1^2}\,e^{\frac{A_4}{2}s},\quad \text{for } s\leq 0;} \tag{54}$$

where A_4 and B_1 are still given in Eq. (36) and Eq. (41a), respectively.

As an interesting new insight of the present derivation, for a Pasternak elastic foundation with $\alpha<-1$, the formula in Eq. (50) provides the opportunity for a second possible moving load velocity value at which a critical damping may be attained, pertaining this time to the rightward wave ($s>0$, B_6=0). The expression of the solution in this case, represented in the complex plane in Fig. 3e, is given as follows for $s\geq 0$:

$$\hat{w}^+_{\beta_{cr}}(s)=\mathrm{i}\hat{F}\,\frac{q_1+q_2-2q_3+(q_1-q_3)(q_2-q_3)\mathrm{i}s}{(q_1-q_3)^2(q_2-q_3)^2}\,e^{\mathrm{i}sq_3},\quad \text{for } s\geq 0; \tag{55}$$

and then its final expression becomes

$$\boxed{\hat{w}^+_{\beta_{cr}}(s)=\hat{F}\,\frac{2A_4+B_3s}{B_3^2}\,e^{-\frac{A_4}{2}s},\quad \text{for } s\geq 0;} \tag{56}$$

where A_4 and B_3 are still given in Eq. (36) and Eq. (41c), respectively.

These occurrences are illustrated in Fig. 6a, where the two-branch curves of critical damping ratio $\zeta_{cr,P}=c_{cr,P}/2\sqrt{k\mu}$ for a Pasternak foundation versus velocity ratio $v/v_{cr,W}$

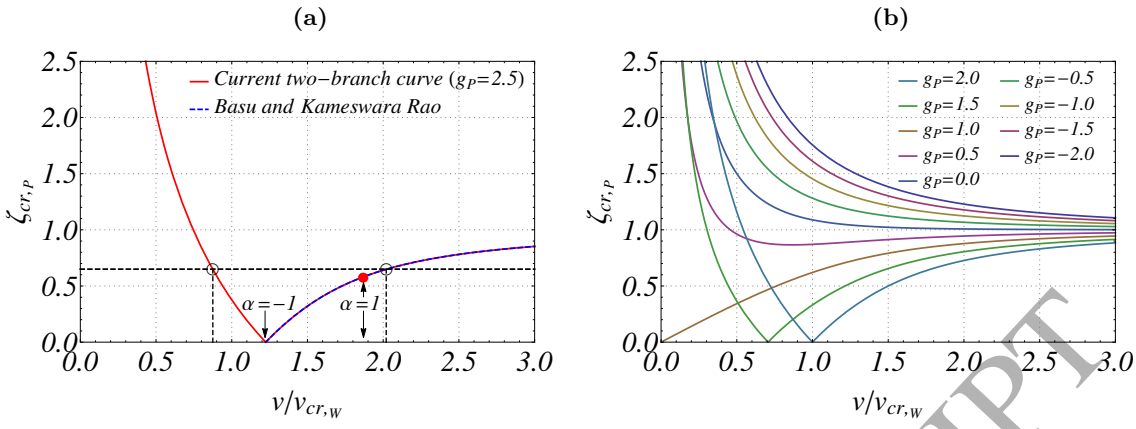

Figure 6: *Two-branch curve of critical damping ratio $\zeta_{cr,P}$ as a function of velocity ratio $v/v_{cr,W}$ (**a**). At a given non-zero value of damping, as that marked by a dashed horizontal line, there always appear two values of velocity for which such damping becomes critical, one for the forward wave (left branch, $\alpha<-1$) and the other for the backward wave (right branch, $\alpha>-1$). The red dot marks the value of critical damping at the critical velocity ($\alpha=1$). Critical damping ratio curves as a function of both velocity ratio $v/v_{cr,W}$ and non-dimensional Pasternak modulus g_P (**b**).*

is depicted. Then, given an arbitrary value of damping, represented in Fig. 6a by a black dashed horizontal line, there exist two distinct values of velocity for which such a value of damping becomes critical, for the forward wave ($\alpha<-1$) and for the backward wave ($\alpha>-1$), respectively. Notice that while such second occurrence had been provided by the formula derived by Basu and Kameswara Rao (2013) [40], the first one was not. In fact, Eq. (49) generalized the formula derived by Basu and Kameswara Rao (2013) [40] for the critical damping ratio, by also providing the first branch of the critical damping curve, by virtue of general character of the present formulation. The dependence of $\zeta_{cr,P}$ on velocity ratio $v/v_{cr,W}$ and non-dimensional Pasternak modulus g_P is also shown in Fig. 6b.

Therefore, on both branches of the critical damping curve, one of the two functions describing the beam-Pasternak foundation response is represented by an exponentially decaying function times a linear function of normalized position from the moving load.

Finally, case $\alpha=-1$, leading to two pairs of double purely-imaginary poles, implies that two new forms (54) and (56) exist simultaneously.

5 Results and interpretation

The explicit universal analytical solution in Eq. (43) reveals that the steady-state response of the beam non-proportionally depends upon both two characteristic system parameters α, β defined in Section 2. According to their definitions provided in Eqs. (9) and (10), the two parameters are in turn functions of moving load velocity v. By combining such definitions, it results that the parametric variation of α and β with the moving load velocity may be represented by parabolas with horizontal axis in the α, β parametric plane.

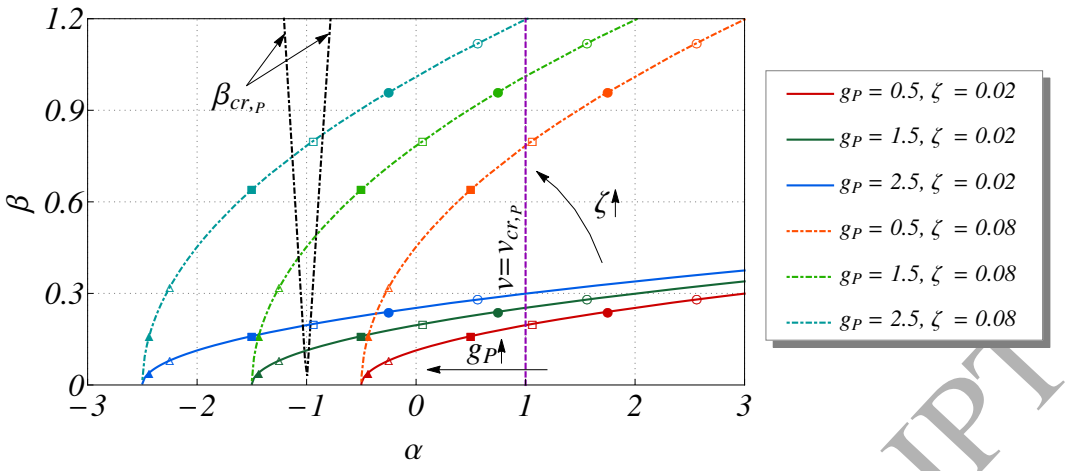

Figure 7: *Graphical representation of the parabolic parametric variation of beam-foundation system parameters α, β as a function of normalized Pasternak modulus g_P, damping ratio ζ and moving load velocity v: ▲ v=0.50 $v_{cr,W}$, △ v=0.75 $v_{cr,W}$, ■ v=1.00 $v_{cr,W}$, □ v=1.25 $v_{cr,W}$, ● v=1.50 $v_{cr,W}$, ○ v=1.75 $v_{cr,W}$. Recall that, from Fig. 5, $v_{cr,P}$=$v_{cr,W}\sqrt{1+g_P}$ at α=1, as marked by the vertical dashed line. For the reference mechanical parameters see Table 2.*

The expression of such parabolas may be written in explicit form as follows:

$$\alpha = \left(\frac{\sqrt{k\mu}/4}{c}\right)^2 \beta^2 - \frac{G_P}{\sqrt{4kEJ}} = \frac{1}{64\zeta^2}\,\beta^2 - g_P; \tag{57}$$

where non-dimensional Pasternak modulus of the foundation g_P, defined in Eq. (11), determines the position of the parabola's vertex, and damping ratio ζ, also defined in Eq. (11), controls the steepness of the parabolas.

Such representation is useful to recognize the type of steady-state response, according to the nature of the poles, which depend on parameters α, β (Fig. 2), i.e. as a function of the characteristic physical parameters of the beam-Pasternak foundation system, as shown in Fig. 7. There, the two branches characterized by a null discriminant (Δ=0) have been represented with a dot-dashed curve. The adopted ranges of parameters employed for the parametric analysis illustrated below have been represented in Fig. 7.

The analysis reported in Section 4 has illustrated that if point (α, β) lies below either the green curve or the red curve in Fig. 2, namely within fields (1) and (3) in Fig. 2, both backward and forward waves are either evanescent or propagating away from the load (source), respectively; on the other hand, if the (α, β) point is placed in the region above both curves, namely within region (2) of the parametric space in Fig. 2, the backward wave becomes evanescent, while the forward wave is propagating. Furthermore, as the (α, β) point approaches the purple half-line in Fig. 2, namely region (6), which is characterized by A_4=0, the exponential decay, ruled by A_4, becomes smaller and smaller; consequently, the range of s with non-negligible wave amplitude is expected to grow, producing waves with very large spatial extension.

Reference mechanical properties of the beam-Pasternak foundation system			
Young's modulus	E	210	GPa
Central moment of inertia	J	3055×10^{-8}	m^4
Mass per unit length	μ	60	kg/m
Winkler foundation modulus	k	250	kN/m^2
Wave number (Winkler foundation)	λ	3141×10^{-4}	m^{-1}
Reference damping coefficient (spring-mass system)	$2\sqrt{k\mu}$	7746	Ns/m^2

Table 2: *Reference mechanical properties of the beam-Pasternak foundation system, assumed for the representations in Fig. 6 and Figs. 8-11.*

To verify the above mentioned a priori considerations and to accurately investigate the effect of the characteristic system parameters on the response behavior, a parametric study can be carried out, at this stage, as reported in the following.

5.1 Response characteristics along the beam

The assumed mechanical properties of the beam and the Winkler foundation modulus have been taken from Castro et al. (2014) [13] and are reported in Table 2. The load is taken acting downward ($F<0$). The normalizing factor in Eq. (2) is now chosen as follows:

$$w_0 = \frac{F}{\lambda^3 EJ}; \tag{58}$$

in order to consistently obtain $\hat{F}=-1$ in Eq. (43).

A graphical representation of the complete normalized response (deflection, rotation, bending moment, shear force) is provided in Figs. 8-11, for various values of moving load velocity v, non-dimensional Pasternak modulus g_P and damping ratio ζ. The considered range of velocities is sufficiently broad, namely it goes from 0.5 to 1.75 times the critical velocity of a beam resting on a Winkler foundation ($v_{cr,W}$). Two values of damping factor have been selected, one indicating a lightly damped system (ζ=2%) and the other a moderately damped system (ζ=8%). Three values of g_P have been assumed (g_P=0.5, 1.5, 2.5), in order to show how this parameter may affect the response of the system.

By observing the curves depicted in Figs. 8-11, some common features of all the represented quantities may be underlined. First, by considering values of α approximately lower than 0.5, corresponding to either a low velocity or a high Pasternak modulus, damping does not affect much the steady-state response, which turns out essentially symmetric with respect to the moving load position. On the contrary, for larger values of α, damping is more effective, both in reducing both wave amplitudes and in changing their phase; in fact, in this case the response becomes noticeably non-symmetric. Secondly, in the presence of propagating waves, by increasing the moving load velocity, the frequency of oscillation of the backward wave decreases (i.e. by having a larger wavelength), while the contrary occurs for the forward wave.

As expected by the definition of α given in Eq. (9), for $\alpha>0$ the effect of the Paster-

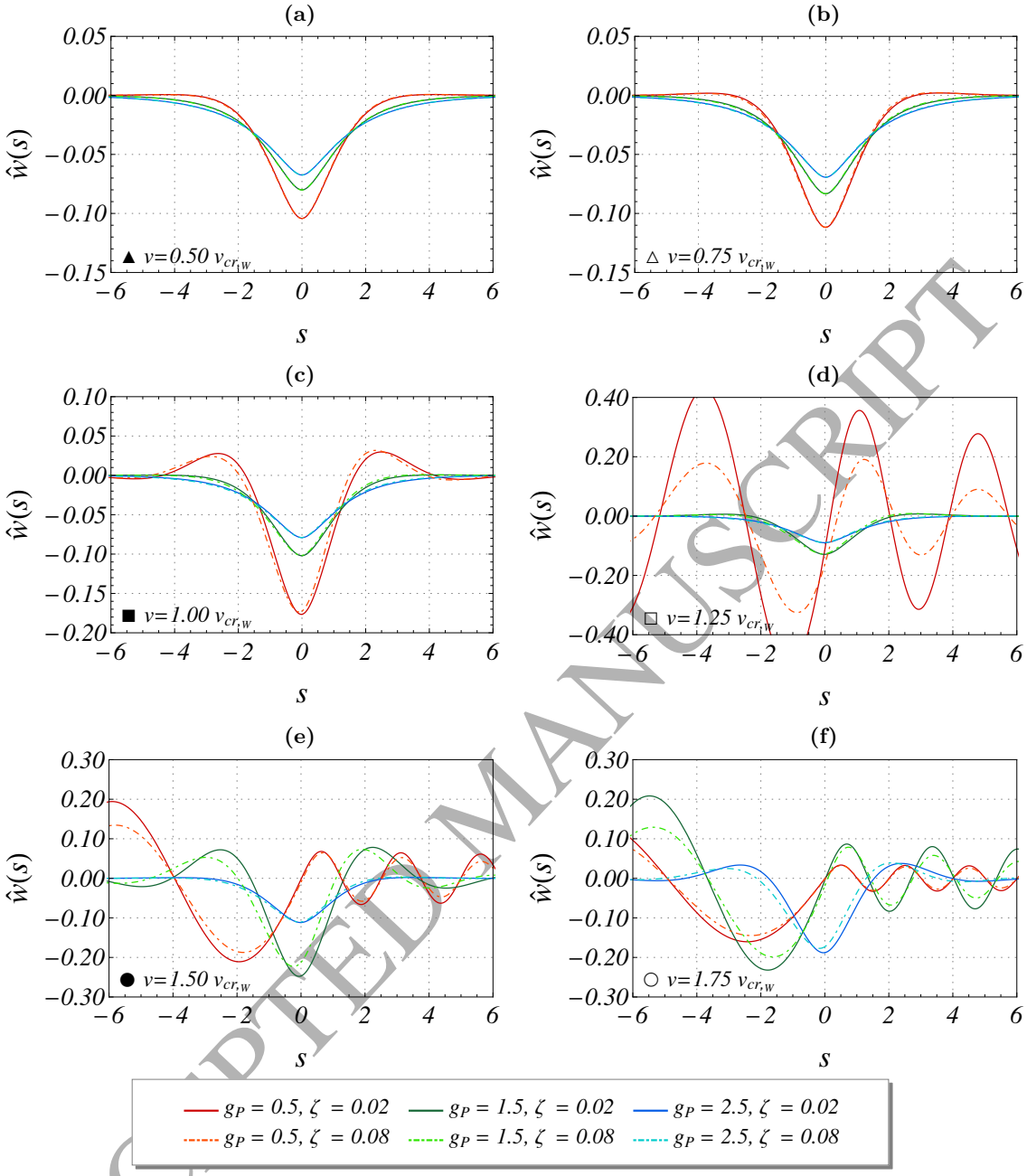

Figure 8: *Normalized deflection $\hat{w}(s)$ for various values of normalized Pasternak modulus g_P and damping ratio ζ at variable moving load velocity v: (**a**) ▲ v=0.50 $v_{cr,W}$; (**b**) △ v=0.75 $v_{cr,W}$; (**c**) ■ v=1.00 $v_{cr,W}$; (**d**) □ v=1.25 $v_{cr,W}$; (**e**) ● v=1.50 $v_{cr,W}$; (**f**) ○ v=1.75 $v_{cr,W}$. For the reference mechanical parameters see Table 2.*

nak modulus may be conceived as to be equivalent to converting the actual moving load velocity into a lower apparent velocity, with the Pasternak modulus being null (Winkler foundation). In addition, when the load velocity is near to the critical velocity (α=1), for instance for the empty square marker on the red line in Fig. 7, the amplitude of the corresponding response quantities grows sharply (see red curves in Figs. 8d-9d-10d-11d).

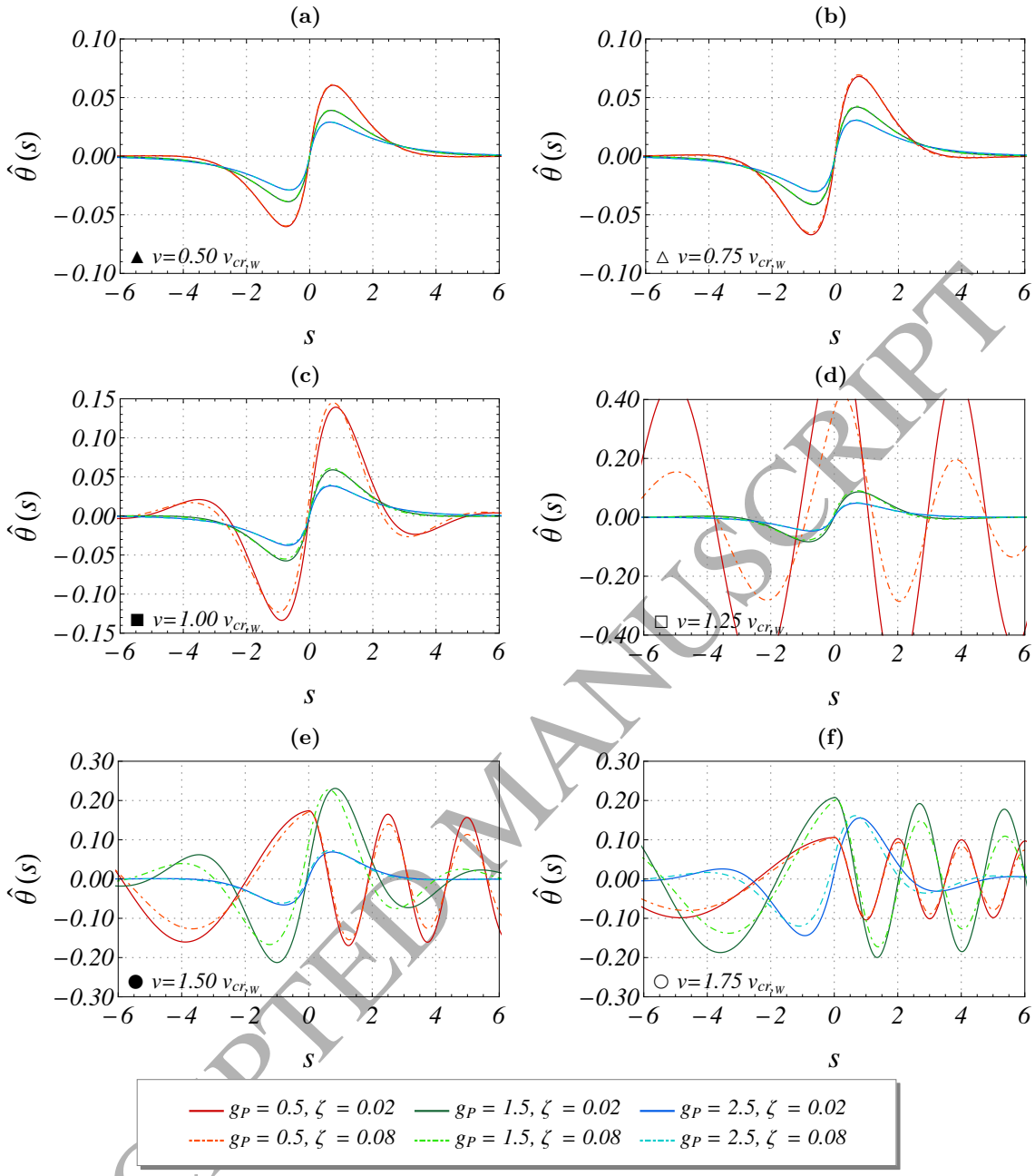

Figure 9: *Normalized rotation $\hat{\theta}(s)$ for various values of normalized Pasternak modulus g_P and damping ratio ζ at variable moving load velocity v: (**a**) ▲ v=0.50 $v_{cr,W}$; (**b**) △ v=0.75 $v_{cr,W}$; (**c**) ■ v=1.00 $v_{cr,W}$; (**d**) □ v=1.25 $v_{cr,W}$; (**e**) ● v=1.50 $v_{cr,W}$; (**f**) ○ v=1.75 $v_{cr,W}$. For the reference mechanical parameters see Table 2.*

By analyzing the normalized deflection shown in Figs. 8a-8f, for either low velocity or high Pasternak modulus (roughly speaking for $\alpha < 0.5$), the results display a downward maximum displacement occurring beneath the moving load position (s=0), analogously to Fig. 5 reported by Kerr's (1972) [27], while as the velocity increases or the Pasternak modulus decreases, the maximum displacements, of the same amount both downward

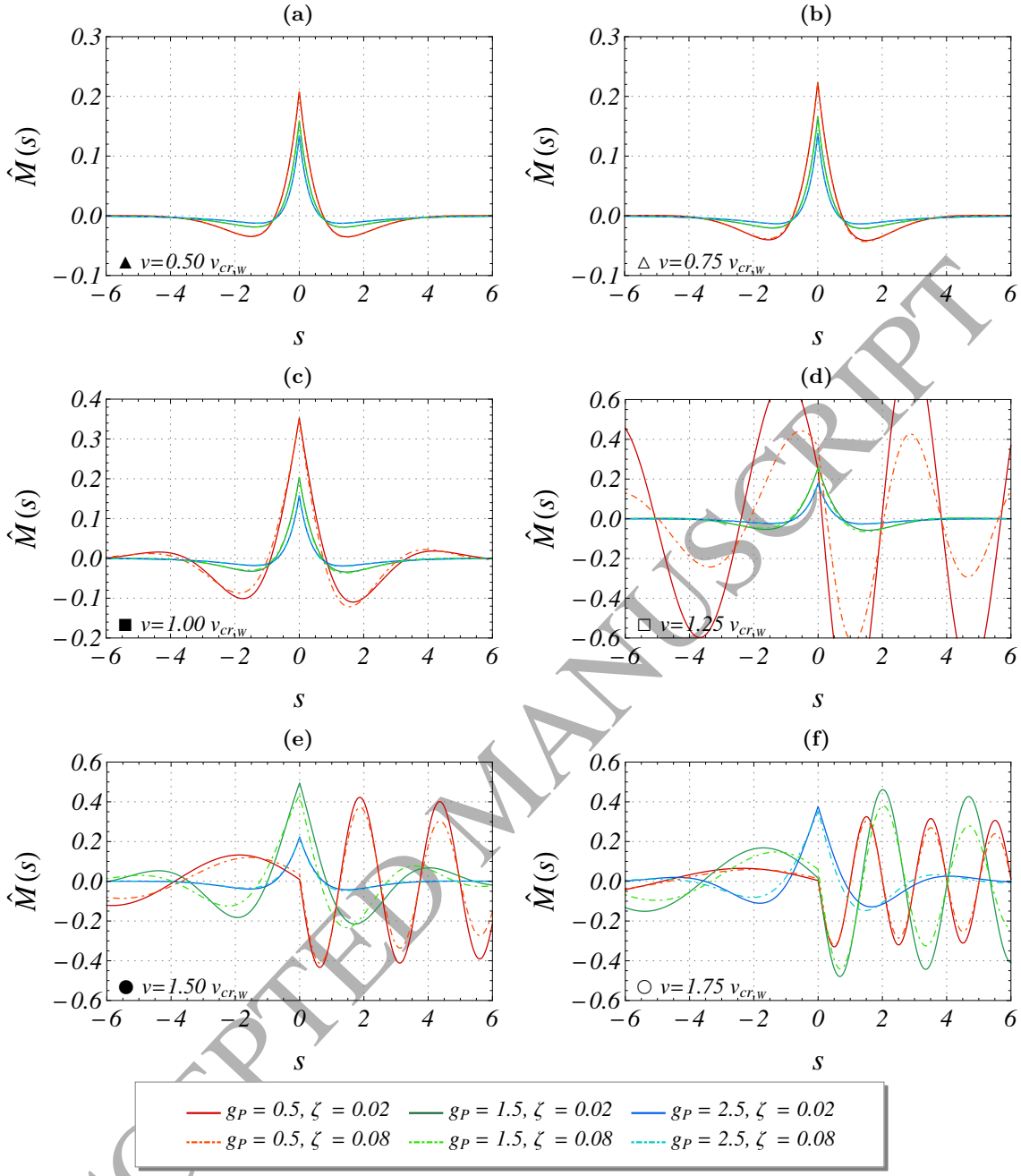

Figure 10: *Normalized bending moment $\hat{M}(s)$ for various values of normalized Pasternak modulus g_P and damping ratio ζ at variable moving load velocity v: **(a)** ▲ v=0.50 $v_{cr,W}$; **(b)** △ v=0.75 $v_{cr,W}$; **(c)** ■ v=1.00 $v_{cr,W}$; **(d)** □ v=1.25 $v_{cr,W}$; **(e)** ● v=1.50 $v_{cr,W}$; **(f)** ○ v=1.75 $v_{cr,W}$. For the reference mechanical parameters see Table 2.*

and upward, appear for a negative value of s, since displacements are larger behind than ahead of the moving load position. Such occurrence does not appear in the plots of the cross-section rotations, shown in Figs. 9a-9f, where a very slight difference between the amplitudes of the two waves may be observed.

Looking at the variations of the normalized bending moment and shear force, the max-

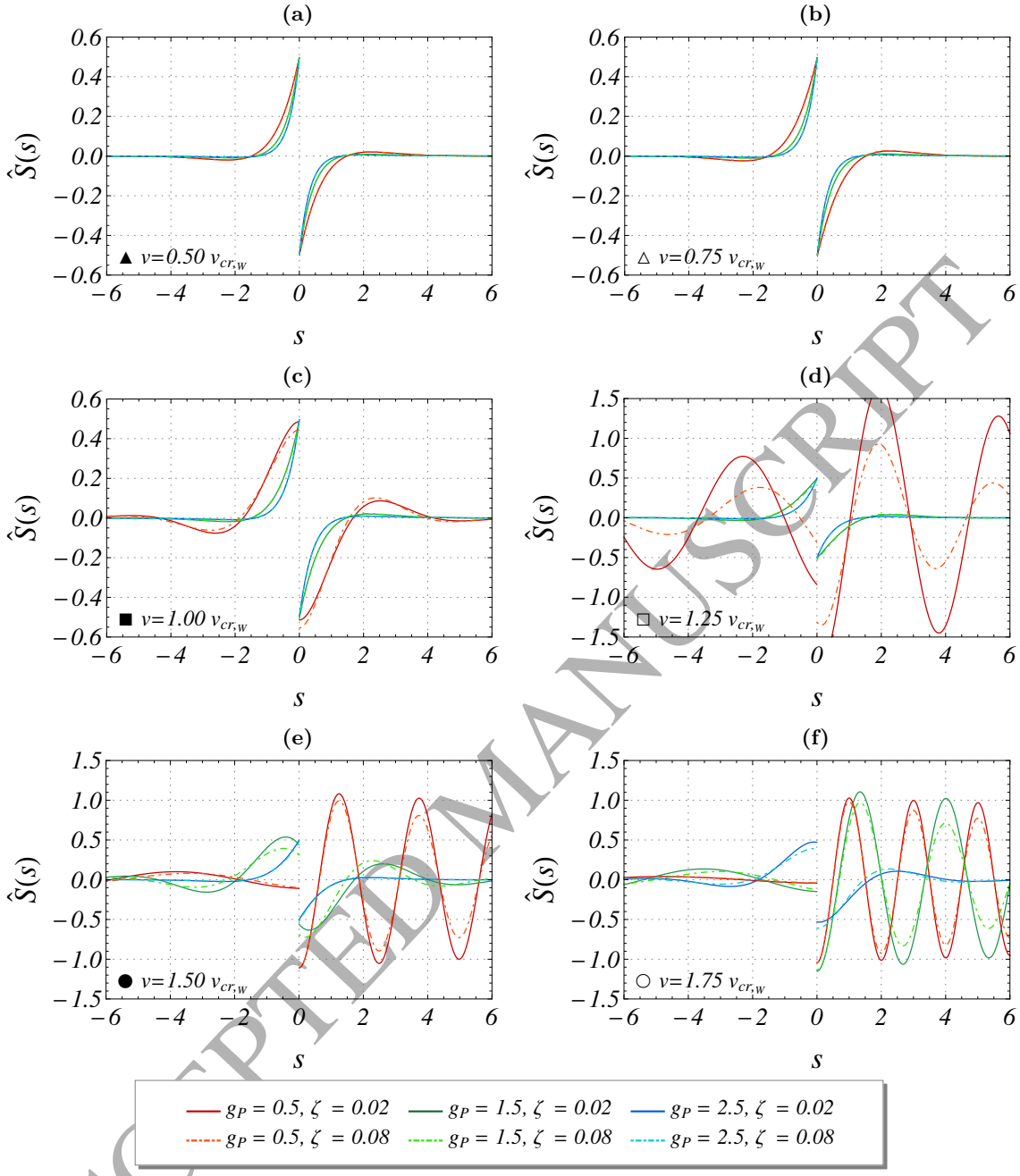

Figure 11: *Normalized shear force $\hat{S}(s)$ for various values of normalized Pasternak modulus g_P and damping ratio ζ at variable moving load velocity v: (**a**) ▲ v=0.50 $v_{cr,W}$; (**b**) △ v=0.75 $v_{cr,W}$; (**c**) ■ v=1.00 $v_{cr,W}$; (**d**) □ v=1.25 $v_{cr,W}$; (**e**) ● v=1.50 $v_{cr,W}$; (**f**) ○ v=1.75 $v_{cr,W}$. For the reference mechanical parameters see Table 2.*

imum is again placed under the moving load for approximately α<0.5, while for larger α a different trend may be captured, with respect to that of the deflection: the maximum values appear on the right of the moving load, that is for s>0. As expected, the bending moment plots in Figs. 10a-10f are continuous and exhibit a kink at the load position (s=0), whereas the shear force curves consistently display a jump discontinuity there.

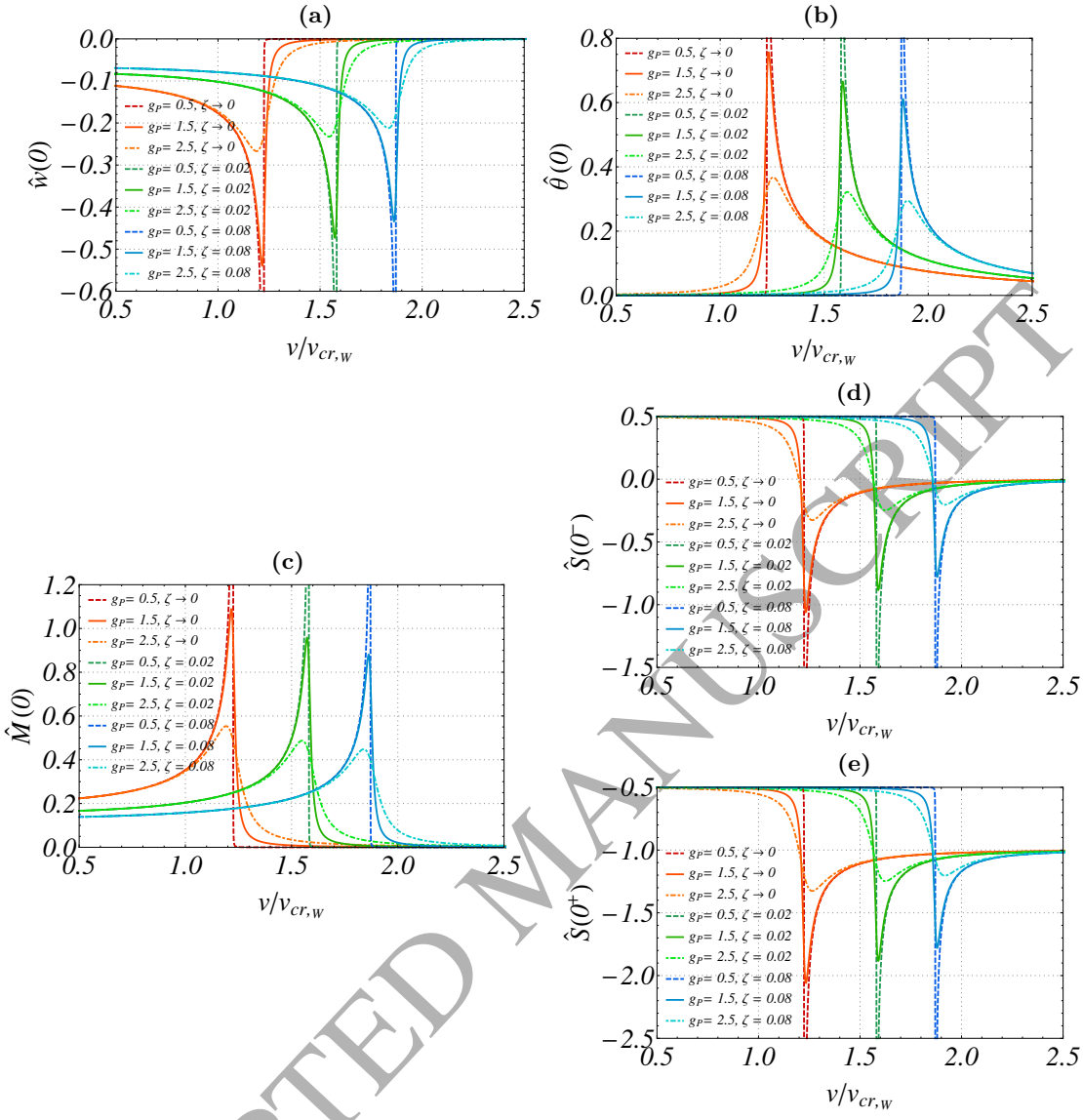

Figure 12: *Variation of normalized deflection $\hat{w}(0)$ (**a**), rotation $\hat{\theta}(0)$ (**b**), bending moment $\hat{M}(0)$ (**c**) and shear forces $\hat{S}(0^-)$, $\hat{S}(0^+)$ (**d**), (**e**) at the point underneath the load (s=0), for various values of normalized Pasternak modulus g_P and damping ratio ζ, at variable moving load velocity v. For the reference mechanical parameters see Table 2.*

5.2 Response characteristics at the point underneath the moving load

Figs. 12a-12c display the normalized response characteristics at the point underneath the load (s=0) provided in Eqs. (44), as a function of the moving load velocity, for various values of non-dimensional Pasternak modulus and damping ratio.

From the observation of these plots, an infinite response may be observed in correspondence of the critical velocity, when approaching the ideal undamped case; on the other hand, a finite peak of response is always displayed in the presence of damping. Regarding the effect of the Pasternak modulus, the already discussed effect of increasing the critical velocity is confirmed also by these latter representations.

Notice that for $\hat{F}<0$ (moving load acting downward), the normalized deflection results always negative ($\hat{w}(0)<0$) as the velocity grows, while both normalized rotation and bending moment remain always positive ($\hat{\theta}(0)>0$, $\hat{M}(0)>0$). The normalized left shear force ($S(0^-)$), initially positive, decreases progressively as the velocity increases, until it changes sign while approaching the supercritical range. On the other hand, the normalized right shear force ($S(0^+)$) remains always negative and for a moving load velocity getting close to the supercritical range its value is even larger than the moving load amplitude, in order to guarantee equilibrium with the left shear force. In case of a zero velocity (static configuration) the load is equally distributed among the left and right shear forces, while in correspondence of the limit situation of velocity going to infinity the load is totally sustained by the shear force acting on the right part of the beam ($S(0^+)$).

The plots of the normalized displacement and bending moment are characterized by an increasing amplitude as the velocity approaches the critical velocities, and by a very steep decrease towards null values at the post-critical conditions. Conversely, the normalized rotation and left and right shear forces display large increments before the critical velocity, and more slowly decrements after passing such a critical value.

In the present analysis, the influence of velocity, damping ratio and Pasternak modulus has been studied. The structural parameters of the beam and the Winkler foundation modulus have been taken as fixed. If one would attempt a parametric analysis involving the latter parameters, it is important to underline that they shall induce a double effect, because they affect not only the normalized response, but also the adopted normalization factors (λ, w_0, θ_0, M_0, S_0). Therefore, in order to analyze the physical sensitivity of the steady-state solution upon variations of such parameters, a non-normalized response or a different type of normalization should be considered.

6 Conclusions

In the present study, the solution of the problem of the steady-state dynamic response of a homogeneous infinite Euler-Bernoulli elastic beam resting on a uniform Pasternak viscoelastic foundation and subjected to a constant point load moving with a constant velocity along the beam has been investigated analytically.

The Fourier transform technique has been applied to derive a universal fully parametric closed-form explicit analytical solution, by means of the theory of complex analysis and the residue theorem. The achieved analytical solution has been summarized in the self-contained chart reported in Fig. 4, which represents a main result of the present investigation.

Furthermore, singular instances of the solution corresponding to a vanishing discriminant of the denominator of the associated Fourier representation, leading to the onset conditions of critical velocity and of critical damping have been consistently derived, analyzed, inspected and interpreted.

Finally, a complete parametric analysis on the effect of the moving load velocity, the

Pasternak modulus and the damping ratio on the beam-foundation response has been developed, for ranges of the parameters spanning a wide spectrum of the parametric space, thus including all possible physical instances. Consistently, extensive representations of the characteristic features of the steady-state response have been provided and discussed.

In conclusion, the developed analytical investigation has drawn several interesting findings concerning the present formulation of the moving load problem. Main achievements of this study may be summarized as follows:

- A rigorous derivation of the general solution by a Fourier transform approach has been obtained, leading to a universal parametric representation of the steady-state response, which depends on two non-dimensional physical parameters of the beam-Pasternak foundation system. The present derivation includes new solution appearances that may be obtained for given values of the physical parameters, such as for a high Pasternak modulus (both positive and negative, the latter interpreted as an axial compression force), outlining a unitary, comprehensive general formulation of the analyzed steady-state moving load problem.
- An a priori characterization on how the beam-foundation response changes according to the paths followed in the space of the system parameters, by varying the moving load velocity, the Pasternak shear modulus and the damping ratio, has been developed by a comprehensive classification of all solution behaviors, based on the parametric nature of the poles of the Fourier transform of the solution. In fact, depending on that, the wave form of the resulting response may present a wide variety of configurations.
- The derived solution turns out to be fully consistent with available solutions reported in the literature, but, with respect to such contributions, the present newly-derived solution constitutes a unified analytical tool endowed of a general validity.
- Moreover, the derived exact solution may be readily used to validate the reliability and accuracy of numerical methods (e.g. FEM modelizations), which may be employed to obtain the response also for more complex problems, where an analytical treatment may not be possible. In this sense, the achieved universal representation resumed in Fig. 4 shall constitute an easily-accessible reference.
- Characteristic features of the steady-state response such as critical velocity and critical damping have been rigorously derived and interpreted. The existence of two branches of the critical damping coefficient, pertaining to each one of the two bending waves (propagating backward and forward) characterizing the beam-Pasternak foundation response, has been revealed.
- In the absence of damping, when the moving load approaches the critical velocity, the beam response becomes unbounded and a steady-state response cannot be attained, neither at the supercritical velocities. The critical velocity for a Pasternak elastic foundation in Eq. (48) is always greater than that for a Winkler elastic foundation in Eq. (12), and quickly raises at increasing Pasternak modulus.
- Similar response features have been deduced from the parametric analysis of the local normalized response characteristics at the moving load position, performed by consid-

ering variable velocity, Pasternak modulus and damping ratio.

- Non-dimensional curves of deflection, cross-section rotation, bending moment and shear force have been presented, showing several important and characteristic features of the structural response. The normalized shapes and amplitudes of these curves are mostly controlled by non-dimensional parameter α in Eq. (9), which in turn depends on the moving load velocity and the Pasternak modulus. Such dependence, together with the effect of damping, as attached to non-dimensional parameter β in Eq. (10), has been widely discussed in the paper.
- As a general consideration, since the Pasternak model shall represent the ground behavior more accurately than the Winkler model, the developed solutions may supply a better guideline for possible ensuing contexts of parameter identification and for practical design purposes.

Acknowledgments

The first two Authors acknowledge public research funding from *"Fondi di Ricerca d'Ateneo ex 60%"* and a doctoral grant and funds at the EAS Department, University of Bergamo.

References

[1] J.T. Kenney Jr., Steady-state vibrations of beams on elastic foundations for moving load, *J. of Applied Mech.*, Transactions of the ASME, **21(4)**, 359–364, 1954.

[2] R.M.S.M. Schulkes, A.D. Sneyd, Time-dependent response of floating ice to a steadily moving load, *J. of Fluid Mech.*, **186**, 25–46, 1988.

[3] V.A. Squire, R.J. Hosking, A.D. Kerr, P.J. Langhorne, *Moving Loads on Ice Plates*, Kluwer Academic Publishers, Dordrecht, The Netherlands, 1996.

[4] Z. Dimitrovová, A.F.S. Rodrigues, Critical velocity of a uniformly moving load, *Advances in Engineering Software*, **50(1)**, 44–56, 2012.

[5] D. Duffy, The response of an infinite railroad track to a moving, vibrating mass, *J. of Applied Mech.*, **57(1)**, 66–73, 1990.

[6] A. Metrikine, H. Dieterman, Instability of vibrations of a mass moving uniformly along an axially compressed beam on a viscoelastic foundation, *J. of Sound and Vibr.*, **201(5)**, 567–576, 1997.

[7] Z. Dimitrovová, New semi-analytical solution for a uniformly moving mass on a beam on a two-parameter visco-elastic foundation, *Int. J. of Mechanical Sciences*, **127**, 142–162, 2017.

[8] L. Frýba, *Vibration of Solids and Structures under Moving Loads, 3rd Edition*, Research Institute of Transport, 1972.

[9] A.D. Kerr, Continuously supported beams and plates subjected to moving loads: a survey, *Solid Mech. Arch.s*, **6(4)**, 401–449, 1981.

[10] H. Ouyang, Moving-load dynamic problems: A tutorial (with a brief overview), *Mechanical Systems and Signal Processing*, **25(6)**, 2039–2060, 2011.

[11] N.D. Beskou, D.D. Theodorakopoulos, Dynamic effects of moving loads on road pavements: a review, *Soil Dynamics and Earthquake Engineering*, **31(4)**, 547–567, 2011.

[12] M. Shamalta, A.V. Metrikine, Analytical study of the dynamic response of an embedded railway track to a moving load, *Arch.s of Applied Mech.*, **73(1)**, 131–146, 2003.

[13] P. Castro Jorge, F.M.F. Simões, A. Pinto da Costa, Dynamics of beams on non-uniform nonlinear foundations subjected to moving loads, *Computers & Structures*, **148**, 26–34, 2014.

[14] P. Castro Jorge, A. Pinto da Costa, F.M.F. Simões, Finite element dynamic analysis of finite beams on a bilinear foundation under a moving load. *J. of Sound and Vibr.*, **346**, 328–344, 2014.

[15] Z. Dimitrovová, Critical velocity of a uniformly moving load on a beam supported by a finite depth foundation, *J. of Sound and Vibr.*, **366**, 325–342, 2016.

[16] Z. Dimitrovová, Analysis of the critical velocity of a load moving on a beam supported by a finite depth foundation. *International Journal of Solids and Structures*, **122–123**, 128–147, 2017.

[17] Y.H. Wang, L.G. Tham, Y.K. Cheung, Beams and plates on elastic foundations: a review, *Progress in Structural Engineering and Materials*, **7(4)**, 174–182, 2005.

[18] D. Froio, E. Rizzi, Analytical solution for the elastic bending of beams lying on a variable Winkler support, *Acta Mechanica*, **227(4)**, 1157–1179, 2016.

[19] D. Froio, E. Rizzi, Analytical solution for the elastic bending of beams lying on a linearly variable Winkler support. *International Journal of Mechanical Sciences*, **128-129**, 680–694, 2017.

[20] K.F. Graff, *Wave Motion in Elastic Solids*, Dover Publications Inc, New York, 1975.

[21] T.E. Simkins, Wave Coupling and Resonance in Gun Tubes, *Technical Report AECCB-TR-89008*, 1–20, 1989.

[22] J.D. Achenbach, C.T. Sun, Moving load on a flexibly supported Timoshenko beam. *Int. J. of Solids and Structures*, **1(4)**, 353–370, 1965.

[23] J.P. Jones, P.G. Buta, Response of cylindrical shells to moving loads, *J. of Applied Mech.*, ASME, **31(1)**, 105–111, 1964.

[24] P.M. Mathews, Vibrations of a beam on elastic foundation, *ZAMM*, **38(3-4)**, 105–115, 1958; II, **39(1-2)**, 13–19, 1959.

[25] D. Froio, R. Moioli, E. Rizzi, Numerical dynamical analysis of beams on nonlinear elastic foundations under harmonic moving load, *Proc. of VII ECCOMAS Conf.*, Crete, Greece, 5–10 June 2016, Paper 7515, 16 pages, ISBN: 978-618-82844-0-1, 2016.

[26] Y.H. Chen, Y.H. Huang, C.T. Shih, Response of an infinite Timoshenko beam on a viscoelastic foundation to a harmonic moving load, *J. of Sound and Vibr.*, **241(5)**, 809–824, 2001.

[27] A.D. Kerr, The continuously supported rail subjected to an axial force and a moving load, *Int. J. of Mechanical Sciences*, **14(1)**, 71–78, 1972.

[28] S. Limkatanyu, N. Damrongwiriyanupap, M. Kwon, P. Ponbunyanon, Force-based derivation of exact stiffness matrix for beams on Winkler-Pasternak foundation, *ZAMM*, **95(2)**, 140–155, 2015.

[29] A.P.S. Selvadurai, *Elastic Analysis of Soil-Foundation Interaction*, Elsevier Scientific Publishing Company, Amsterdam, 1979.

[30] V.Z. Vlasov, U.N. Leontiev, *Beams, Plates, and Shells on Elastic Foundations* (translated from Russian), Israel Program for Scientific Translations, Jerusalem, 1966.

[31] W. Stadler, R.W. Shreeves, The transient and steady-state response of the infinite Bernoulli-Euler beam with damping and an elastic foundation, *The Quarterly J. of Mech. & Applied Mathematics*, **23(2)**, 197–208, 1970.

[32] J.P. Sheehan, L. Debnath, On the dynamic response of an infinite Bernoulli-Euler beam, *Pure and Applied Geophysics*, **97(1)**, 100–110, 1971.

[33] H. Saito, T. Terasawa, Steady-state vibrations of a beam on a Pasternak foundation for moving loads, *J. of Applied Mech.*, **47(4)**, 879–883, 1980.

[34] M.H. Kargarnovin, D. Younesian, Dynamics of Timoshenko beams on Pasternak foundation under moving load, *Mech. Research Communic.s*, **31(6)**, 713–723, 2004.

[35] D. Younesian, M.H. Kargarnovin, Response of the beams on random Pasternak foundations subjected to harmonic moving loads, *J. of Mechanical Science and Technology*, **23(11)**, 3013–3023, 2009.

[36] H. Ding, K.L. Shi, L.Q. Chen, S.P. Yang, Dynamic response of an infinite Timoshenko beam on a nonlinear viscoelastic foundation to a moving load, *Nonlinear Dynamics*, **73(1)**, 285–298, 2013.

[37] W. Stadler, The general solution of the classical problem of the response of an infinite plate with an elastic foundation and damping, *J. of Elasticity*, **1(1)**, 37–49, 1971.

[38] K. Watanabe, Response of an elastic plate on a Pasternak foundation to a moving load, *Bulletin of the Japan Society of Mechanical Engineers*, **24(191)**, 775–780, 1981.

[39] A.K. Mallik, S. Chandra, A.B. Singh, Steady-state response of an elastically supported infinite beam to a moving load, *J. of S. and Vibr.*, **291(3)**, 1148–1169, 2006.

[40] D. Basu, N.S.V. Kameswara Rao, Analytical solutions for Euler-Bernoulli beam on visco-elastic foundation subjected to moving load, *Int. J. for Numerical Analytical Methods in Geomechanics*, **37(8)**, 945–960, 2013.

[41] C.Y. Cao, Y. Zhong, Dynamic response of a beam on a Pasternak foundation and under a moving load. *J. of Chongqing University*, **7(4)**, 311–316, 2008.

[42] R.U.A. Uzzal, R.B. Bhat, W. Ahmed, Dynamic response of a beam subjected to moving load and moving mass supported by Pasternak foundation, *Shock and Vibr.*, **19(2)**, 205–220, 2012.

[43] N. Evcan, A. Hayir, Dynamic response of a infinite beam on a Pasternak foundation and under a moving load, *Proc. of VII ISEC-7 Conf.*, Honolulu, 18–23 June 2013, 79–83, ISBN: 978-981-07-5354-2, 2013.

[44] A. Ghani Razaqpur, K.R. Shah, Exact analysis of beams on two-parameter elastic foundations, *Int. J. of Solids and Structures*, **27(4)**, 435–454, 1991.

[45] S.A. Eftekhari, A differential quadrature procedure for linear and nonlinear steady state vibrations of infinite beams traversed by a moving point load, *Meccanica*, **51(10)**, 2417–2434, 2016.

[46] M. Hetényi, *Beams on Elastic Foundation*, The University of Michigan Press, Ann Arbor, USA, 1946.

[47] R.G. Buschman, *Integral Transformations, Operational Calculus, and Generalized Functions*, Springer, Dordrecht, 1996.

[48] D.G. Duffy, *Transform Methods for Solving Partial Differential Equations, 2nd Edition*, Chapman & Hall/CRC, London, UK, 2004.

[49] J. Bak, D.J. Newman, *Complex Analysis*, Springer, New York, USA, 2010.

[50] E.L. Rees, Graphical discussion of the roots of a quartic equation, *The American Mathematical Monthly*, **29(2)**, 51–55, 1922.

[51] Wolfram Research Inc., Mathematica, Champaign, IL, User Guide.

[52] L.E. Dickson, *Elementary Theory of Equations*, John Wiley & Sons, New York, 1914.

[53] E.B. Vinberg, *A Course in Algebra*, American Mathematical Society, Providence, Rhode Island , USA, 2003.